Journal Pre-proofs

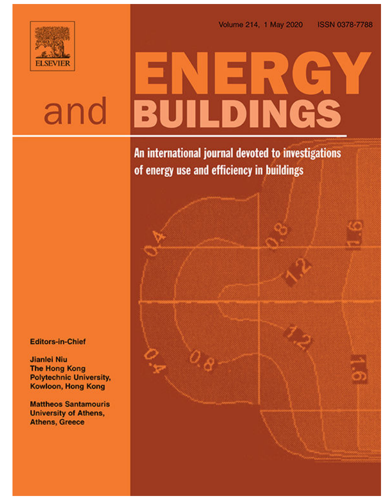

Operation and energy flexibility evaluation of direct load controlled buildings equipped with heat pumps

Gerard Mor, Jordi Cipriano, Benedetto Grillone, Frédéric Amblard, Ramanunni Parakkal Menon, Jessen Page, Marcus Brennenstuhl, Dirk Pietruschka, Ruben Baumer, Ursula Eicker

PII: S0378-7788(21)00768-4
DOI: https://doi.org/10.1016/j.enbuild.2021.111484
Reference: ENB 111484

To appear in: *Energy & Buildings*

Received Date: 3 August 2021
Accepted Date: 16 September 2021

Please cite this article as: G. Mor, J. Cipriano, B. Grillone, F. Amblard, R.P. Menon, J. Page, M. Brennenstuhl, D. Pietruschka, R. Baumer, U. Eicker, Operation and energy flexibility evaluation of direct load controlled buildings equipped with heat pumps, *Energy & Buildings* (2021), doi: https://doi.org/10.1016/j.enbuild.2021.111484

Operation and energy flexibility evaluation of direct load controlled buildings equipped with heat pumps

Gerard Mor[a], Jordi Cipriano[a,*], Benedetto Grillone[b], Frédéric Amblard[c], Ramanunni Parakkal Menon[d], Jessen Page[c], Marcus Brennenstuhl[e], Dirk Pietruschka[e], Ruben Bäumer[f], Ursula Eicker[d]

[a]*Centre Internacional de Mètodes Numèrics a l'Enginyeria. Building Energy and Environment Group. Pere de Cabrera 16. Office 2G. 25001. Lleida. Spain*
[b]*Centre Internacional de Mètodes Numèrics a l'Enginyeria. Building Energy and Environment Group. Rbla. Sant Nebridi 22, 08222 Terrassa, Spain*
[c]*Hes-So Valais-Wallis. Route du Rawyl 47. 1950 Sion, Switzerland*
[d]*Next Generation Cities Institute, Concordia University, 1455 Boulevard de Maisonneuve O., EV-6.111 Montréal H3G 1M8, Canada*
[e]*Stuttgart University of Applied Sciences, Schellingstraße 24, 70174 Stuttgart, Germany*
[f]*Centrica Business Solutions Belgium NV. Roderveldlaan 2/b2, 2600 Antwerp, Belgium*

Abstract

To date, the assessment of the energy flexibility to be delivered by existing buildings and by their legacy HVAC systems is hindered by a lack of commonly agreed-upon methodologies. There are many research works in the field; however, many of them are focused on the design stage or, in case of addressing building operation, they are based on controlled experimental setups. The novelty of this paper lies in the fact that it develops and validates an original methodology for the Flexibility Function estimation to evaluate the delivered energy flexibility of several Automated Demand Response services applied on different heat pump systems working under real operations. The active interaction with several electricity markets, ranging from the Spanish day-ahead market to the German and Swiss ancillary services markets, have also been evaluated during the winter and spring seasons. The method results showed that heat pumps could offer a significant potential of flexibility in the analysed countries. Nevertheless, it has also been envisaged that some restrictions concerning reaction times and reliability may affect its readiness for certain ancillary services markets.

Keywords: demand response, HVAC, flexibility, model predictive control

*Corresponding author
Email addresses: gmor@cimne.upc.edu (Gerard Mor), cipriano@cimne.upc.edu (Jordi Cipriano), bgrillone@cimne.upc.edu (Benedetto Grillone), frederic.amblard@hevs.ch (Frédéric Amblard), ramanunniparakkal.menon@concordia.ca (Ramanunni Parakkal Menon), jessen.page@hevs.ch (Jessen Page), marcus.brennenstuhl@hft-stuttgart.de (Marcus Brennenstuhl), dirk.pietruschka@hft-stuttgart.de (Dirk Pietruschka), Ruben.Baumer@centrica.com (Ruben Bäumer), ursula.eicker@concordia.ca (Ursula Eicker)

Nomenclature

Acronyms

$aFRR$ automatic Frequency Restoration Reserve Market

AR AutoRegressive

ARX AutoRegressive with eXogenous

$ASHRAE$ American Society of Heating, Refrigerating and Air-Conditioning Engineers

BaU Business as Usual

BES Building Energy Simulation

CM Cluster Manager

$CVRMSE$ Coefficient of Variation of the Root Mean Squared Error

DA Day-Ahead Electricity Price

DER Distributed Energy Resource

DHW Domestic Hot Water

DR Demand Response

DSO Distribution System Operator

ECM Energy Conservation Measures

EU European Union

FCR Frequency Containment Reserve

FF Flexibility Function

HP Heat Pump

IoT Internet of Things

$MAPE$ Mean Absolute Percentage Error

$mFRR$ Manual Frequency Restoration Reserve

MPC Model Predictive Control

$NEMO$ Nominated Electricity Market Operator

$NLME$ Non Linear Mixed Effect

$RMSE$	Root Mean Squared Error
RR	Reserve Replacement
SAR	Seasonal Auto Regressive
SH	Space Heating
SVM	Support Vector Machines
TS	Time Series
TSO	Transmission System Operator

Subscripts and superscripts

b	baseline
bd	building number
e	active
f	trace to be tracked
o	outdoor
opt	optimized
t	time t

Variables

A	Percentage of activation time within a time step
B	Backward shift operator
i	flexibility evaluation period
n	number of time steps
P	Power
RC	Resistor and Capacitator
T	Temperature

1. INTRODUCTION

Renewable energy sources like solar panels and wind turbines are invaluable for transitioning to a fossil-free energy system to mitigate climate change impacts. However, their natural fluctuations introduce significant uncertainty in the power grid. In addition, they transform the present unidirectional centralized system into a bi-directional decentralized system with smaller units and multiple prosumers, increasing the difficulty to achieve power balance [1]. This leads to an increased need for flexibility on the demand side [2, 3] and for new storage capacity [4, 5]. One attractive solution identified to support the transition of power systems is to manage not only the energy supply but also the demand via Demand Response (DR) programs [6, 7]. The principle behind it is to use various economic incentives to shift the electrical loads of end-use customers from times with a high wholesale market price or when the system's security is threatened to other time periods. As has been pointed out in [8], there are predominantly two types of DR programs: i) explicit DR (also called incentive-based); ii) and implicit DR (also called price-based). In Implicit DR, a price signal is sent to the prosumers to motivate their user behaviour change. Explicit DR involves the participation of a third party, who takes action on behalf of a customer by sending an activation signal such that the system behaviours are directly modified. In both DR programs, and considering that nearly 50 % of the total energy consumption of buildings comes from Space Heating (SH)/Cooling (SC) and domestic hot water (DHW), as stated by [9], there is definitely a role that electrically driven Heating, Ventilation and Air Conditioning (HVAC) systems can play.

Although the installation of control devices, communication, control protocols and standardization have improved, DR is currently still rarely implemented in the commercial and even less in the residential sector in Europe [10]. Serale et.al [11] reviewed 161 papers on Model Predictive Control (MPC) in buildings, and revealed that only a fourth considered residential buildings and only a bit more than a fifth compared experimental cases to simulated cases. Kohlhepp et.al. [12] performed a thorough review of 16 projects of field tests and demonstrations of applied DR from around the world. Only four projects had more than 100 households, a size large enough to represent load diversity and test resource competition. A singular case of commercially applied DR to large scale residential buildings is run by the French company Voltalis, which manages one of the biggest portfolios of explicit DR services in the world. They follow a strategy of DR based on service curves [13, 14].To our knowledge, they have not published peer-reviewed papers analysing the impacts of this DR strategy or provided a general methodology to evaluate the delivered energy flexibility. In general, there is a lack of test case benchmarks. Comparing the results among case studies with different goals, addressed electricity markets and technology environments is still very challenging.

The few real case applications of DR have brought forth a wide diversity of methodologies to evaluate the energy flexibility that individual or clustered buildings can provide. In many cases, assessment methodologies are focused on the potential energy flexibility at the building design stage. Arteconit et. al [15] is a clear example of defining an indicator of flexibility labelling at the design stage. Finck et. al [16] performed a very detailed analysis of the demand flexibility that power-to-heat systems can deliver. Several flexibility indicators such as available storage capacity and efficiency are enhanced with a flexibility factor, which relates electricity costs in the lower price and higher price periods in a day-ahead electricity market DR scenario. A thermal instantaneous power flexibility indicator is also described. These indicators have a great potential to evaluate the energy flexibility in DR services addressing the ancillary markets. The only weakness is that they were demonstrated in a theoretical simulated environment. Moreover, that research was more focused on developing control strategies and not on the flexibility evaluation itself.

In their hands-on review, Reynders et.al [17] made a valuable contribution in reviewing prior research dealing with definitions and quantification of energy flexibility. One of their main conclusions was that a large share of the performed research practices did not explicitly define or were not focused on quantifying energy flexibility. Yet, they dealt with the development of control strategies and algorithms for specific case studies. They also stated that most of the studies had in common the identification of three general properties of energy flexibility: i) the potential flexibility in several time horizons; ii) the load which can be shifted; and iii) the cost of this flexibility. The authors also deducted that methodologies aimed at quantifying the energy flexibility by analyzing triggered events at specific times have greater strengths when dealing with the flexibility to be delivered by the thermal mass of buildings or energy storage systems. In contrast, methodologies which relied on differences in the accumulated energy profiles are difficult to interpret because they treat systems driven by multiple time constants as a single state system. El Geneidy and Howard [18] performed a detailed analysis of the categories of characteristics that constrain the contracted flexibility potential in homes. Although their results are valuable for defining further DR strategies, they are limited by simplified assumptions and exclusively based on simulated scenarios. Bampoulas et.al [19] conducted a more detailed recent review on studies aiming at defining suitable flexibility indicators. They highlighted that most of these studies were limited to evaluating control strategies and assessing the activating and deactivating of the building's thermal mass. Still, they did not clearly quantify the flexibility potential of HVAC systems.

Following these remarks, Junkers et.al [20] developed a novel methodology to characterize the energy flexibility as a dynamic function named the Flexibility Function (FF). This FF enables a Flexibility Index, which describes how a building can respond to certain activation signals. The FF is a step-response function that assumes that the relation between the penalty signal and the power load is linear and time-invariant. Several theoretical cases were presented to validate this proposed FF, demonstrating how the FF enables the quantification of the energy flexibility in different types of buildings. This paper represents a valuable contribution to the field since it establishes a robust methodology to represent, in a normalized manner, the correlation between the penalty signal and the load response. The concept of the FF applies to several building typologies and DR scenarios but specifically addresses implicit DR services. However, the assumption that the dependence of the active power and the activation variable is linear limits its applicability to DR services which can fulfil this requirement. Recently, Junkers et.al [21] published a paper presenting a new generic method capable of overcoming the linearity and time dependency of the correlation between the flexibility and the penalty signal. This new method follows the principles of the *FF*, but it changes the perspective. They developed a non-linear dynamic model based on stochastic differential equations. It is applied to price-based controlled buildings and water towers, showing high robustness, accuracy and scalability to similar business cases. One limitation is that these methods are developed to specifically address implicit DR services driven by penalty signals triggered by one of the stakeholders of the electricity sector. This is very common in many electricity markets, such as the spot electricity market, the intra-day market, or certain ancillary services markets. However, in some explicit DR services, where the activation variable is a power trace to be followed, such as when a commercial aggregator makes bilateral agreements with their Balance Responsive Parties (BRP), both the *FF* and the flexibility characterization model defined in [20, 21] need to be modified or extended to adapt them to these different kinds of activation variables.

In our research, an extension of the previously developed flexibility characterization procedures is performed, which is the main novelty of the research work. Based on the background knowledge developed by Junkers et.al [20], and further improved in [21], new linear regression-based models, designed to characterize the energy flexibility delivered by blocks of buildings, are developed and validated in real cases. These new flexibility models address different implicit and explicit DR scenarios. For example, the activation variable can be the spot market price, the percentage of power to be activated, or a power trace to be tracked. This is also an extra contribution to the paper. One last novelty of the research lies in the fact of developing and applying these flexibility models on clustered residential buildings, ranging from high energy performance detached houses (Germany) to building blocks connected to low-temperature district heating (Switzerland) or a group of buildings formed by small shops, a food market and residential units (Spain). In all the scenarios, the methods were applied to remote-controlled heat pumps with different system configurations.

The rest of the paper is organized as follows. Section 2 describes the developed methodology, identifies potential flexibility markets, presents a common methodology for quantifying energy flexibility and describes the models and the new *FF* formulations. Hereinafter, the three case studies (Spain, Germany and Switzerland) are presented in Section 3. They comprise three clusters of buildings with heat pumps remotely driven by MPC procedures. The operation of the DR services and the results are summarized in Section 4, where details of the outcomes of the different direct load control tests are presented. The energy flexibility is assessed, through the derived Flexibility models and Flexibility Functions, in this section. Finally, the findings are extensively discussed in Section 5, and summarised in Section 6. Furthermore, some perspectives for future work are also envisaged in Section 7.

2. Methodology

2.1. Identification of the addressed flexibility markets

Different markets exist for the trading of electricity between buyers and sellers. In the day-ahead market, products are traded for delivery on the following day. The intraday market trades products to balance possible deviations from the day-ahead forecast. Balancing or control reserves markets are needed to balance electricity generation and consumption in the short term. Three different types of control reserves markets are available: i) Frequency Containment Reserve (FCR), ii) Automatic Frequency Restoration Reserve (aFRR), and iii) Manual Frequency Restoration Reserve (mFRR). They differ according to the principle of activation, to their bid minimum size and symmetry, and their activation speed. The last category of markets is the Reserve Replacement (RR) market. These capacity mechanisms aim at ensuring the security of supply from a long-term perspective.

In this paper, four of the above-mentioned markets are selected to be addressed through direct load control DR services: i) the Spanish wholesale electricity market (day-ahead); ii) the German operating reserve; iii) the German intraday spot market and; iv) the Swiss imbalance market (aFRR).

In Spain, OMIE is the nominated electricity market operator (NEMO) for managing the Iberian Peninsula's day-ahead and intraday electricity markets. The delivery takes place on the day after the trading day (incl. weekends or holidays), and trading sessions take place in one daily auction 365 days/year. Sale and purchase bids can be made considering between 1 and 25 energy blocks in each hour, with power and prices offered in each block. In the case of sales, the bid price increases with the block number; in purchases, the bid price decreases with the block number. The minimum size is 0.1 MW. The Spanish TSO, Red Eléctrica Española, has developed an information system known as 'System Operator Information System (esios)', specially designed to run all the necessary processes to ensure economic and reliable exploitation of the Spanish Power System in real-time. The esios portal offers an open API where the wholesale electricity prices for the next 24 h are published once the spot market is closed (at 13 h of every day). These electricity prices become the control variable for the direct load control services implemented in the Spanish use case.

Unlike the day-ahead spot market in Germany and Switzerland, the intraday market can be described as a corrector market because the time intervals between trade and activation and the activation period are significantly lower. Thereby, electrical energy is traded in intervals of one hour for Switzerland or 15 min for Germany. In Germany, trades for 15 min intervals can be completed between 15:00 (CET) of the previous day until 5 min before activation [22].

In Germany, four different TSOs are responsible for the reserve markets, and around 60 companies are pre-qualified to deliver operating reserves. Therefore, compared to the spot trade market, there is a highly reduced field of actors. The FCR activation time of a few seconds is very short term. aFRR requires an activation time of less than 30 s and 5 min to reach full power. RR requires 5 min for activation. mFRR and RR are traded daily and bids can be provided in blocks of 4 h. Negative and positive reserve power is traded. As a first instance, positive or negative power is offered with different assigned prices. If an offer is accepted, a working price (e.g. EUR/MWh) is also offered, and the activation occurs according to the working price within a merit order list. The main drawbacks of mFRR and RR are that at least 1 MW of power must be certified. Thereby, an aggregated larger pool operation is necessary. The German operating reserve market, especially mFRR has seen dropping costs within the last years [23, 24], whereas in comparison the amount of energy traded at the EPEX Intraday market has almost doubled from 2014 – 2019 (from 47 TWh to 91.6 TWh) [25], shifting the favourability more to intraday trade. In the German pilot site, activations were carried out by Centrica, an aggregator company situated in Belgium, according to available market data from Belgium. This is justifiable due to the fact, that the spot market products are tradable in between Germany and Belgium [26] as well as the operating reserve market conditions are comparable [27].

The Swiss operating reserve markets are managed only by one TSO (Swissgrid). Compared to Germany, the minimum certified bid of the aFRR and RR markets is 5 MW, making them even less accessible for residential buildings, as a vast pool of assets would be needed. For aFRR, the trading is automated. The products traded are asymmetric and must be available 30 s to 5 min after the notification for a duration of up to 15 min. The size of the aFRR in Switzerland in 2017 was ±380 MW [28]. The high participation of hydropower supply in the reserve markets limits residential DR. The high number of DSOs present in Switzerland [28], each of them with a limited asset pool, also hinders the development of DR services by the DSOs. For the field tests of the Swiss pilot site, the targeted reserve market was the aFRR, as its market constraints are the most accessible for heat pumps. By combining a pool of batteries with fast activation time and heat pumps whose power availability lasts longer, an aggregator could theoretically fulfil the market constraints. The trading in this work was done by Centrica (aggregator), and HES-SO Valais-Wallis carried out the activations in Switzerland. Real trading could not be tested, as it would have required 200 times the capacity offered by the pilot site to reach the minimum bid of 5 MW.

2.2. *New reference methodology to assess energy flexibility*

The methodology to characterize the energy flexibility in a more standardized way follows the initial methodology set out by [20]. This methodology defines a dynamic function, named the flexibility function FF, which characterizes the energy flexibility of any device through the use of penalty signals. In our research, the analysed use cases do not strictly follow the activation of the energy flexibility through penalty signals since they respond to other DR schemes. To address these different DR schemes, we took a broader approach than [20] and implemented a methodology to include other kind of signals and activation variables which are more realistic for the analysed energy flexibility markets. The proposed methodology follows the process shown in Fig. 1. As can be seen, the initial point starts with setting up the baseline modelling, which corresponds to the energy performance model of the buildings in a Business as Usual (BaU) scenario. This baseline model is then used to forecast the building energy consumption for the time horizon defined by the activation period. This energy forecasting is integrated into a model predictive control optimization where the activation variable is the output. The cost function depends on the flexible electricity market to be addressed. The activation period is different for each use case and flexible electricity market. It is driven by the optimized activation variable, ranging from a penalty signal, such as the day-ahead price, a percentage of power activation time, or a power trace to be tracked. The active power consumed throughout of activation period is registered. This time series is considered as the dependent variable within the flexibility model. The baseline forecasting and the activation variable time series are defined as the independent variables. The flexibility model is then formulated also to include the corresponding autoregressive terms. The next step consists of training this flexibility model with historical data of the activation period. Once the flexibility model is trained and validated, the i-step prediction is used to define the flexibility function, FF.

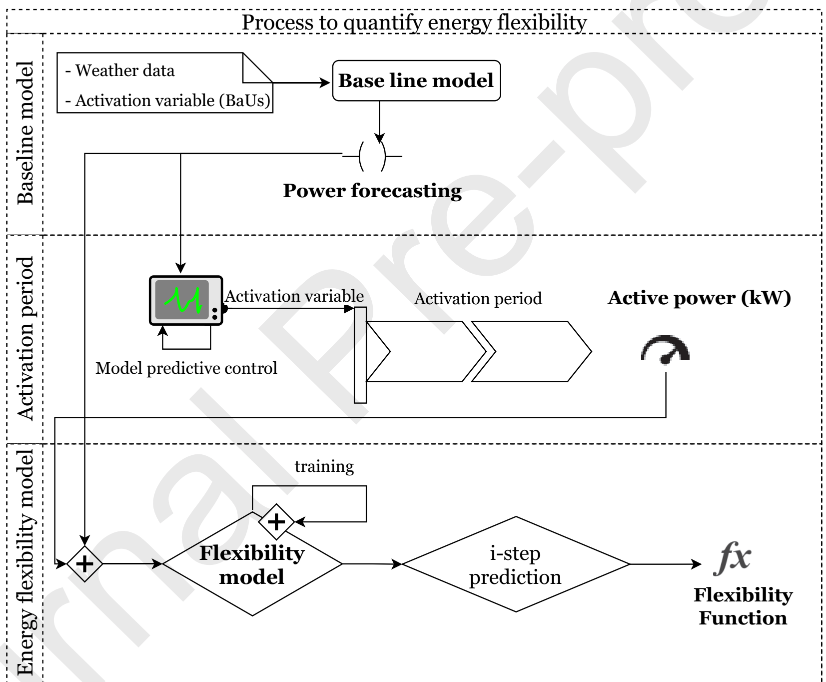

Figure 1 – The general process to quantify the energy flexibility

.

2.2.1. *Baseline modelling*

Since the energy flexibility cannot be directly measured, as it represents the activation or deactivation of power usage, it is determined by comparing measured power during the activation period and forecasting the power consumed by the building as if the activation had not taken place. This supposed scenario is called the Business as Usual (BaU) scenario. To determine the energy load forecasting under the BaU scenario, a model of the thermal dynamics and the energy consumption of the building, prior to the activation period, needs to be developed. This model is called the baseline model. The baseline model can be defined as the energy characterization of the starting situation and has a fundamental role in the determination of energy flexibility. In fact, the baseline model allows isolating the effects of the activation variables from the effects of other parameters that can simultaneously affect the energy consumption. To obtain the baseline model, several approaches can be followed:

- Empirical modelling based on a system of differential equations and heat transfer functions
- Grey box modelling based on state-space models
- Data-driven modelling based on transfer function models or machine learning techniques

In this research, the three approaches have been used for the different use cases. The first approach requires detailed models with several monitored variables and a calibration stage to fit with the monitored data. An example of these kinds of calibration processes can be found in [29]. The second approach requires monitoring the state variable (indoor temperature or water tank temperature) and a precise process to identify the unknown parameters. A[30, 31] detailed description of the identification procedure applied over suitable grey box building heat dynamics models is presented. The third approach requires good data quality of a minimum historical period and the measurement of the control variable. Several authors applied this last approach to determine the heat dynamics of buildings. In [32], some of the most common data-driven methods used to develop baseline models are reviewed. The baseline models developed in each use case are described in detail and referenced in the corresponding subsection of Section 3 of this document.

2.2.2. Flexibility models

A flexibility model is a regression-based model which aims at finding the correlation among the active power, the activation variable and the power under the BaU scenario. In this research, a data-driven approach is followed based on Autoregressive (AR) models. As previously mentioned, the initial modelling technique is defined by [20] is modified to adapt it to the specific constraints of the different activation variables. The original model by Junker et al. assumes that the active load when exposed to a the penalty signal can be separated into two parts; the load that dynamically responds to the the the penalty, and the non-responsive load (baseload power, in our equations). However, in our case the dynamics due to the active and baseload signal itself are added. Thus, an ARX model is considered based on the initial equation presented in [20]. This allows to better estimate the amount of time and load that can be flipped once an activation, a change of price, or a trace to follow is received. Additionally, it helps to the proper estimation of the rebound effect caused by a change in the penalty, as it considers the thermal inertia available in the system.

In the use cases when the activation variable is the day-ahead electricity price of the wholesale spot market, the model formula is described in Eq. 1.

$$\phi_{T_o}(B)P_t^e = \omega_{T_o}(B)P_t^b + \Psi_{T_o}(B)DA_t + \varepsilon_t \quad (1)$$

The auto regressive terms $\phi_{T_o}(B)$, $\omega_{T_o}(B)$ and $\Psi_{T_o}(B)$ are the parameters of the model. The sub index T_o represents their dependence with one categorical variable, the outdoor temperature. In order to better express this dependency, a 4 hours moving-averaged transformation is applied over the outdoor temperature for the testing periods. This averaged temperature is further split in two levels: [6.67 °C - 12.3 °C] and [12.3 °C - 21.5 °C]. Therefore, the T_o is not used as a exogenous variable of the model. The backward shift operators,B, are defined as $B^k y_t = y_{t-k}$, where y_t is the considered variable (P_t^e, P_t^b,DA_t) at time t and $k \in [0, j]$. Here, j refers to the maximum order allowed to that backward shift operator, B. DA_t corresponds to the activation variable, the day-ahead electricity price. The ε_t corresponds to the white noise residual of the model at time t.

In the use cases when the activation variable is the percentage of activation time within each time step, the model formula is described in Eq. 2.

$$\phi_{bd}\big(B\big)P_t^e = \omega_{bd}\big(B\big)P_t^b + \Psi_{bd}\big(B\big)A_t + \varepsilon_t \tag{2}$$

The auto regressive terms $\phi_{bd}(B)$, $\omega_{bd}(B)$ and $\Psi_{bd}(B)$ are the parameters of the model. The sub index bd represents their dependence with one categorical variable, the building number. bd comprises the categorical values of the building number for this use case [20, 22, 24, 25], and a virtual building that aggregates the power of all of them. Therefore, the building number, bd, is not used as a exogenous variable of the model. The backward shift operators,B, are defined as $B^k y_t = y_{t-k}$, where y_t is the considered variable (P_t^e, P_t^b,A_t) at time t and $k \in [0, j]$. Here, j refers to the maximum order allowed to that backward shift operator, B. A_t corresponds to the activation variable, which is the percentage of time, within every time step, with active power, $A_t = [0\% - 100\%]$. The ε_t corresponds to the white noise residual of the model at time t.

In the use cases when the activation variable is a trace to be tracked, the power used within the activation period is no longer the model's dependent variable. In Eq. 3, the dependent variable is substituted by the difference between the active power, P_t^e, and the baseline power,P_t^b. The activation variable in Eq. 1 is then substituted by the difference between the power trace to be tracked, P_t^f and the baseline power, P_t^b. The modified formula is shown in Eq. 3.

$$\phi_{s,T_o}\big(B\big)\big(P_t^e - P_t^b\big) = \omega_{T_o}\big(B\big)\big(P_t^f - P_t^b\big) + \varepsilon_t \tag{3}$$

The autoregressive terms $\phi_{s,T_o}(B)$, $\omega_{T_o}(B)$ are the parameters of the model. The sub-index T_o represents their dependence on a categorical variable, the outdoor temperature. Based on a 4 hours moving-averaged transformation of the outdoor temperature, for the test periods, the results are split into two groups of outdoor temperature levels: [6.5 °C - 15.7 °C] and [15.7 °C - 28.5 °C]. The sub-index s refers to the sign of the trace to be tracked in relation to the baseline power, being equal to 1 when it is positive, equal to 0 when there is no difference with the baseline power, and equal to -1 when it is negative. Therefore, neither the T_o nor the s are used as exogenous variables of the model. The backward shift operators,B, are defined as $B^k y_t = y_{t-k}$, where y_t is the considered variable (P_t^e, P_t^b,X_t) at time t and $k\epsilon[0,j]$. Here, j refers to the maximum order allowed to that backward shift operator, B. The ε_t corresponds to the white noise residual of the model at time t.

2.2.3. Flexibility Functions

The Flexibility Function (FF) can be understood as the impulse response function of each flexibility model since the flexibility models include autoregressive terms of the dependent variables, which cause an influence over the P_t^e when $t \geq 1$. To do so, an i-step prediction is performed to estimate the impulse response of the models properly.

In the use case when the activation variable is the day-ahead price, the FF is determined based on a positive and a negative change in the day-ahead electricity price (±0.1 €/kWh) for the time steps n = 15, 60 and 120 minutes and for a flexibility evaluation period of i = 480 minutes. When the activation variable is the percentage of time of activation within each time step, 100 % activation signals for time steps of n = 1, 2 and 4 hours are tested along a flexibility evaluation period of i = 12 hours. Both use cases follow a similar procedure to determine the FF:

$$t = \left(0, 1, ..., i\right) \tag{4a}$$

$$P_{t\leq 0}^e = 0 \tag{4b}$$

$$P_{t\epsilon\mathbb{N}}^b = 0 \tag{4c}$$

For the day-ahead electricity price as the activation variable:

$$DA = \begin{cases} 0.1, & \text{if positive price change} \\ -0.1 & \text{if negative price change} \end{cases} \tag{4d}$$

$$DA_t = \Big(\underbrace{0, (DA, .., DA)}_{n\ times}, \underbrace{(0, ..., 0)}_{n\text{-}i\ times}\Big) \tag{4e}$$

$$\Phi_{k=0}^b\big(B\big)P_t^e = -\Phi_{k\geq 1}^b\big(B\big)P_t^e + \Psi^b\big(B\big)DA_t \tag{4f}$$

$$\Phi_{k=0}^b\big(B\big) = 1 \tag{4g}$$

$$FF_t = P_t^e = -\Phi_{k\geq 1}^b\big(B\big)P_t^e + \Psi^b\big(B\big)DA_t \tag{4h}$$

For the percentage of time activation within a time step as the activation variable:

$$A_t = \Big(\underbrace{0, (100, .., 100)}_{n\ times}, \underbrace{(0, ..., 0)}_{n\text{-}i\ times}\Big) \tag{4i}$$

$$FF_t = P_t^e = -\Phi_{k\geq 1}^b\big(B\big)P_t^e + \Psi^b\big(B\big)A_t \tag{4j}$$

In the use case when the activation variable is a trace to be tracked, the FF is determined by considering a 100 % activation signal of time steps n = 15, 30 and 60 minutes for a flexibility evaluation period of i = 120 minutes. A multi-step prediction method is used to predict the expected response of ±1 kW of the trace to be tracked. The previous estimate of the flexibility function, $(P^e - P^b)$, is used for the new prediction step. The baseline power is set to

$P_t^b = 0$ for $t \in (0, 1, ..., i)$. Here, s is equal to 1 if the activation is pos equal to -1 if it is negative.

$$\left(P^e_{t\le0} - P^b_{t\le0}\right) = 0 \tag{5a}$$

$$\left(P_t^f - P_t^b\right) = \begin{cases} 0, & \text{if } t \le 0 \\ \Big(\underbrace{(s, ..., s)}_{n\ times}, \underbrace{(0, ..., 0)}_{i\text{-}n\ times}\Big), & \text{otherwise} \end{cases} \tag{5b}$$

$$\Phi_{s,T_o}(B)\left(P_t^e - P_t^b\right) = \omega_{T_o}(B)\left(P_t^f - P_t^b\right) \tag{5c}$$

$$\Phi_{s,T_o k=0}(B)\left(P_t^e - P_t^b\right) = -\Phi_{s,T_o k\ge1}(B)\left(P_t^e - P_t^b\right) + \omega_{T_o}(B)\left(P_t^f - P_t^b\right) \tag{5d}$$

$$\Phi_{s,T_o k=0}(B) = 1 \tag{5e}$$

Considering the flexibility model of Equation 3 and the set up described in previous equations, the FF is defined as:

$$\begin{aligned} FF_t &= \left(P_t^e - P_t^b\right) \\ &= -\Phi_{s,T_o k\ge1}(B)\left(P_t^e - P_t^b\right) + \omega_{T_o}(B)\left(P_t^f - P_t^b\right) \end{aligned} \tag{6}$$

3. Case studies

The methodology to evaluate the energy flexibility is applied over three case studies which have in common a direct load control of space heating systems driven by heat pumps:

- Case study of the Spanish wholesale electricity market price as the activation variable. Blocks of buildings placed in North-East Spain (Sant Cugat)
- Case study of the percentage of activation time as the activation variable. Residential households placed in South Germany (Wüstenrot)
- Case study of a trace to be tracked as the activation variable. Blocks of residential buildings placed in Switzerland (Naters)

A new player, called the Cluster Manager (CM), is incorporated in these case studies. CMs are site managers that cluster together with the local energy , which are remotely controlled (e.g. heat pumps). They have technical knowledge of these energy systems and the connected devices (control system, meters, sensors...). They manage these assets and act as the bridge between the aggregator, who bid in the markets, and the end-user. Thus, they do not have to deal with market specifications handled by the aggregator.

3.1. Spanish case study: wholesale market price

This case study is a pilot site constituted by buildings that combine apartments, offices, shops and a local food market. They are placed in a city called Sant Cugat, in Northern East Spain. Figure 2 shows the space heating and cooling system configuration. It comprises a water storage tank of 3,500 litres fed by two reversible heat pumps accounting for 60 kW of electric power. The heat pumps are controlled by an immersed temperature probe inserted into the bottom of the water tank. The heat pumps deliver thermal energy to the water storage tank through a primary circuit with two hydraulic pumps and external heat exchangers, which follow the same operation schedules as the heat pumps. The water tank provides hot and cold water to two different hydraulic circuits, which transfer this thermal energy to 32 offices, 3 shops and a local food market. These hydraulic circuits are managed by two 3-way motorized valves incorporating a proportional integral derivative (PID) control, leading to variable water volume flow rates. The control variable of the system is the water tank setpoint temperature. Since the two heat pumps do not have variable-speed compressors, they are thermostatically controlled in ON/OFF modes.

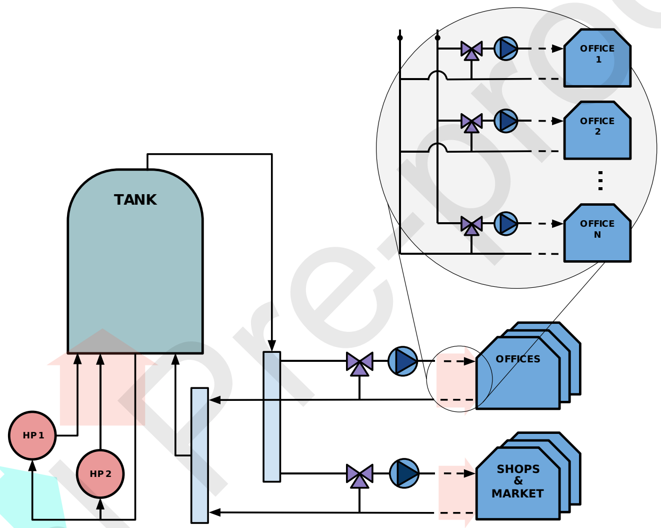

Figure 2 – Space heating configuration of the Spanish use case. The zoom shows details of the hydraulic distribution ring

.

The direct load control strategy followed in this use case is based on the augmented heat pumps performance with price information from the wholesale market and weather forecast data for the current and following day. The heat pumps' electrical use adjusts times when the Spanish wholesale market spot price is lower (day-ahead optimization). To make these services operational, a Model Predictive Control (MPC) approach is put into practice. Every day at 00:00, a Genetic Algorithm (GA) optimizes the cost function, which is the minimum daily electricity consumption cost and gets the vector of the setpoint temperature of the water storage tank, T^s_{opt}, for the next 24 hours in the more cost-effective way.

The baseline model is developed based on the third approach mentioned in Section 2.2.1. It is a data-driven approach formed by two ARX models. They define the dynamic energy balance between the electricity load of the heat pumps, the water tank temperature and the thermal energy delivered to the offices, to the shops and the local food market, as well as the thermal losses in the water storage tank and the water distribution rings. More details of this kind of model can be found in [33]. These two forecasting models need, as inputs, day-ahead predictions of the thermal energy consumed by the shops, the offices, and the local food market. Since they form a block of buildings, they can be simplified as a multi-space building formed by several thermal balance nodes. This model is expected to behave highly non-linear in relation to the external temperature and other climate-dependent exogenous variables. Therefore, data-driven models are also used to evaluate their energy performance. After a previous fine-tuning phase, where several machine learning models were evaluated, the Generalised Additive Model GAM, developed by Hastie et.al [34], provided the highest accuracy and was the selected one.

3.2. German case study: percentage of activation time

This case study is a pilot site situated in the rural municipality of Wüstenrot in southwest Germany. It consists of a newly built positive energy settlement with 18 residential single and multifamily buildings. These buildings are connected to a low-temperature district heating grid fed by a so-called "agrothermal" – a large scale geothermal - collector. All buildings are equipped with decentralized heat pumps, thermal buffer storage tanks ranging from 175 to 300 litres, radiant floor systems, and photovoltaic (PV) systems of installed power between 6 and 29 kWp per building. In addition, a cloud-based monitoring system is installed for 12 buildings that include all relevant thermal and electrical energy flows. Within those 12 buildings, a local energy management system is installed to control the heat pumps. Figure 3 shows a scheme of the energy systems configuration of one of the households. Since different manufacturers provided the heat pumps, some connectivity problems appeared with the interfaces of some of them and the activation was only carried out for four heat pumps manufactured by Tecalor (Typ TTF 10 and TTC05). Two of these heat pumps have a maximum electrical power of 2.38 kW, and two have a maximum power of 3.82 kW. These activations aimed to test the potential and challenges of flexible control of heat pumps from the viewpoint of a flexible service provider.

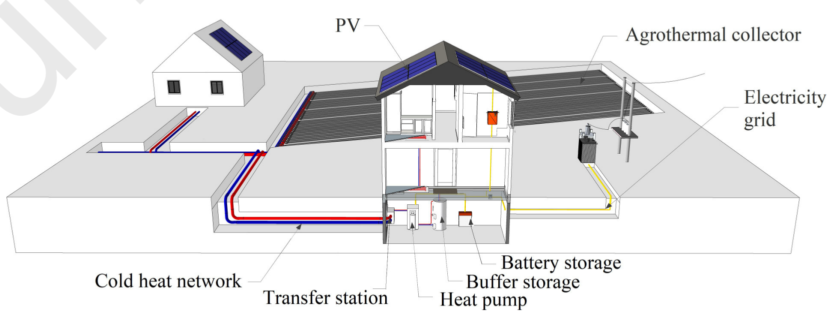

Figure 3 – Energy systems configuration of one of the single households of Wüstenrot pilot site

The development of the baseline model followed the first approach mentioned in Section 2.2.1. For four of the selected households, a white-box model of each building was generated. More details of the models can be found in

[35] and in [36]. They include heat pumps, buffer storage water tanks and control systems. To increase the model's accuracy, a calibration on parameters changeable by the users (indoor setpoint temperature and air exchange rate) with measured data was carried out. Given the unavailability of a baseline for the fifth household, due to inadequate monitoring data, this baseline has been derived from another house which was most similar (same heat pump type and no heating buffer) applying a linear extrapolation based on the historical consumption difference of both. Input parameters for the heat pump control are active power, DHW temperatures and floor heating temperatures. The control strategy is a direct load control over heat pumps on/off.

3.3. Swiss case study: trace to be tracked

This case study is a pilot site placed in the municipality of Naters, in Southern Switzerland. It comprises 12 residential multi-family buildings connected to a centralized low-temperature district heating network (anergy network). It represents 166 residential units. The size of the buildings ranges from 4 to 36 residential units per building. The buildings' construction years range from 1919 to 2015. Thus their envelopes have different thermal efficiencies and have either radiators or floor heating systems. Each building is equipped with one or two fixed speed compressor heat pumps, thermal buffer storage tanks for SH and DHW. Hardware components called 'gateways' are installed in each building. They collect, process and export data from the building devices (e.g. heat pumps, electricity meters) to a cloud-based platform that enables remote control of the heat pumps. The gateways installed in this use case do not have the same level of internal intelligence as the management system installed in the German use case. Due to some restrictions in the control interfaces with the heat pumps, only five out of fourteen heat pumps were intensively tested, accounting for a maximum aggregated electricity power of 34.3 kW. Figure 4 shows and scheme the energy systems configuration of the multi-apartment buildings.

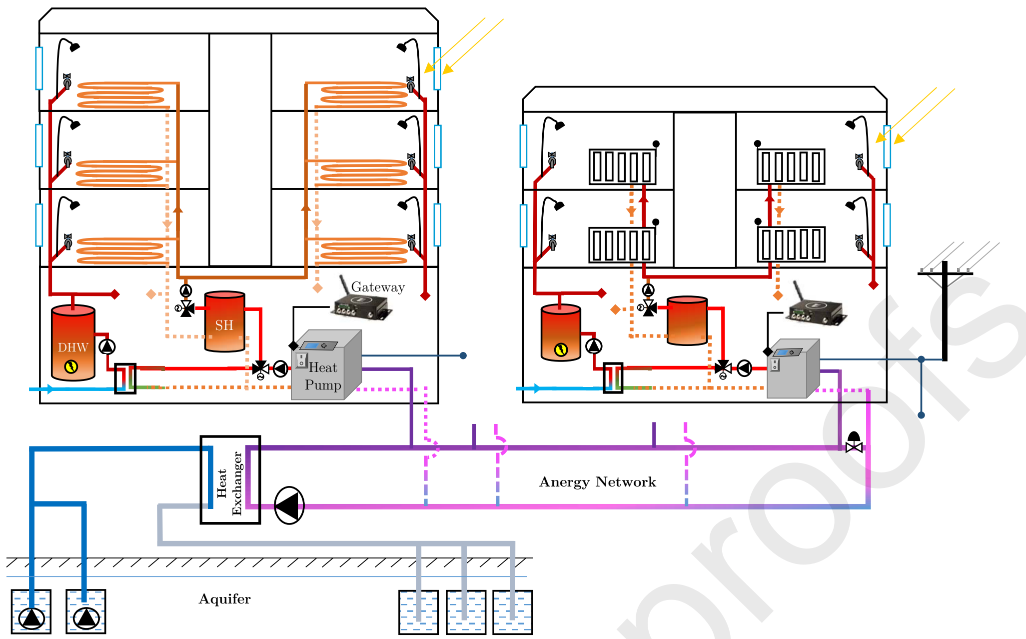

Figure 4 – Energy systems configuration of one of the multi-apartment buildings of Nater's pilot site

The test aims to confirm the potential and challenges of flexible control of heat pumps in residential buildings from the viewpoint of a flexible service provider. A transactive DR approach was tested (a two-way communication system). Its reliability and performance over consecutive days with multiple DR-events per day was also assessed. The framework can be divided into three steps: i) the site is waiting to provide DR services by running BaU; ii) the aggregator starts negotiating power traces with the CM; iii) once a trace has been agreed on, the CM tracks it with an MPC adapted from the formulation developed by [37]. The baseline trace is modelled based on the third approach mentioned in Section 2.2.1. It is a data-driven approach formed by a Seasonal Autoregressive model (SAR) for each building using the past 3 days' power data. The aggregated baseline for the site is computed by summing up the estimated baseline of each building. The other traces are generated by solving scheduling optimization problems. The control variables of the heat pumps are the SH and DHW temperature set points, which are increased/decreased based on the new values optimized by the MPC.

4. Results

4.1. Operation of the Spanish case study

Figure 5 depicts the results of the direct load control applied in the case study where the Spanish wholesale spot market price acts as the activation variable. An MPC optimization was applied during the activation period, which comprised from March 29th to April 12th 2020.

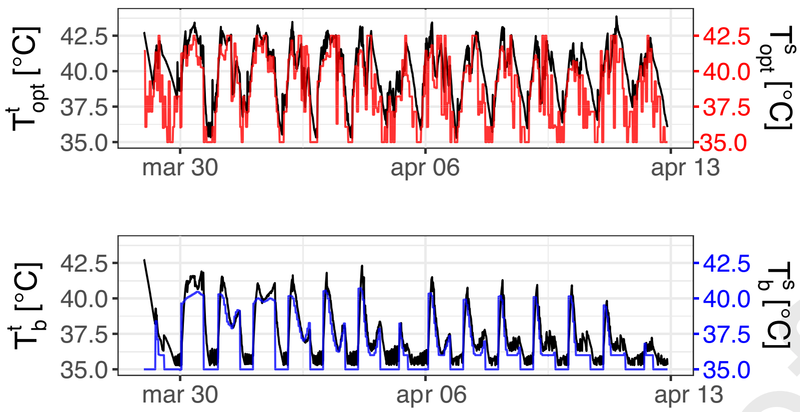

Figure 5 – Results of the direct load control of the use case of the Spanish wholesale spot market price as activation variable

The upper figure shows, in a black-coloured line, the monitored active water storage tank temperature,T^t_{opt} along the activation period. It is compared with the water storage tank setpoint temperature,T^s_{opt}, the red-coloured line, obtained as the output of the day-ahead optimization performed every day. The T^s_{opt} is the direct control variable that drove the heat pumps performance along the activation period. As can be seen, the water tank temperature follows the optimized setpoint temperature very well. The lower plot shows the simulated baseline forecasting of the water storage tank temperature (black-coloured line), T^t_b, and the corresponding setpoint temperature (blue-coloured line), T^s_b, in the BaU scenario, which is minimum operational temperature level required by the offices, shops and local food market to keep the comfort requirements. The differences in both plots show the effect of the activation. It can be seen that the baseline forecasting usually has two temperature peaks and a second smaller temperature level. In contrast, the optimized temperature shows a single peak that is slightly lagged in time. This time lagging shows the MPC is shifting the higher setpoint temperature values to the periods with lower electricity prices.

4.1.1. Time series inputs for the flexibility model development

In Figure ,6 the day-ahead signal price, DA, the forecasting of the baseline power load,P^b, and the active power of the heat pumps,P^e, are shown. Comparing the two time series of power, the differences due to the MPC are appreciable. The bigger differences can be seen for the first days of April, where the active power is concentrated in the lower price hours while the baseline forecasting also consumes in higher prices periods.

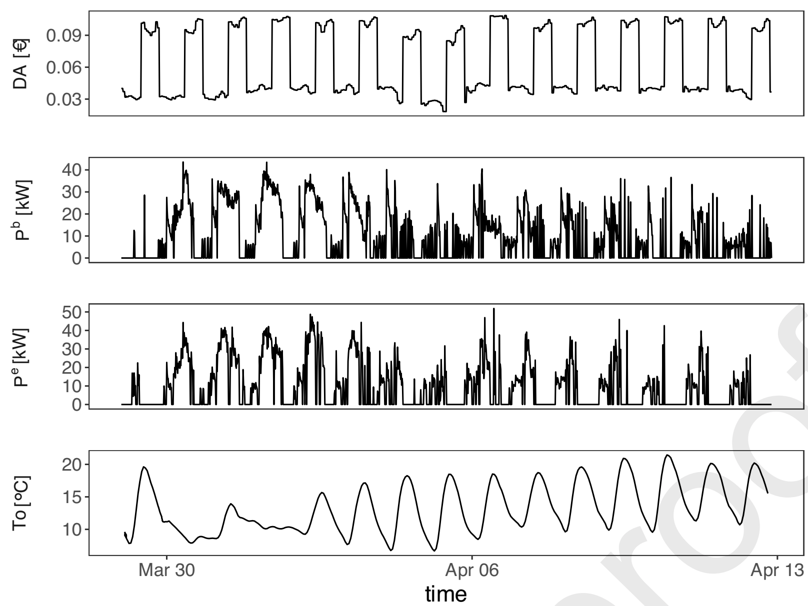

Figure 6 – Active power, P^e, forecasting of the power baseline, P^b, day-ahead electricity price, DA and outdoor temperature, T_o of the heat pumps of the Spanish use case, during the direct load control operation period

Since the objective of this use case is to reduce the cost of the energy consumption of the heat pumps, Figure 7 depicts the accumulated cost difference achieved between the active optimized energy performance (black line) and the BaU scenario (red line). The reduction of cost reaches 18 % at the end of the field test operation period. This is an auspicious outcome to consider day-ahead price optimization as an important way to optimize the operational costs of heat pumps systems while offering flexibility to the electricity system.

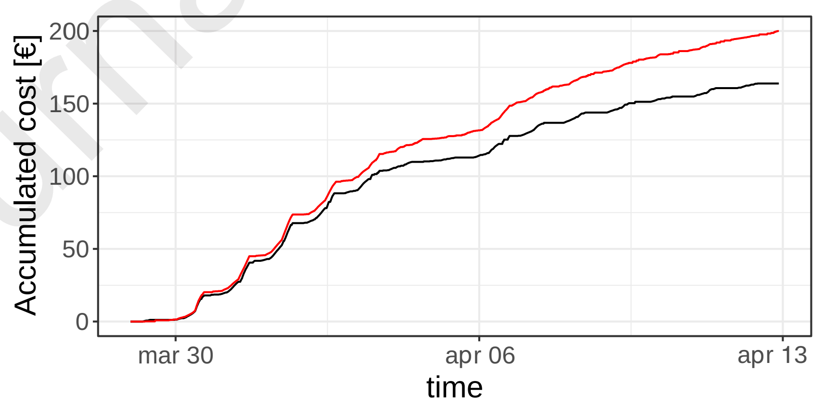

Figure 7 – The accumulated cost of the active optimized energy performance (black line) compared to the BaU scenario (red line)

4.2. Operation of the German case study

Before operating the Tecalor heat pumps, different tests were conducted to verify their control capabilities. An upwards signal of 100 % activation for

30 minutes, followed by a stop of 10 minutes and the second activation of 15 minutes was sent to the heat pump controller. The result is shown in Figure 8. The time to start up was 56 seconds from the setpoint to on. Besides, the heat pump needed 15 minutes to reach 75 % of the maximum power. It can also be seen that the activation profile started with a first step increase, followed by a roughly linear ramp. The time to shut down was 1 min 22 seconds, whereas the shutting down profile was a decreasing step function. There is a 20-minute recovery time between switching off and switching the heat pump on again. These factors determine how a flexibility service provider can control the heat pump flexibly and integrate it into a virtual power plant.

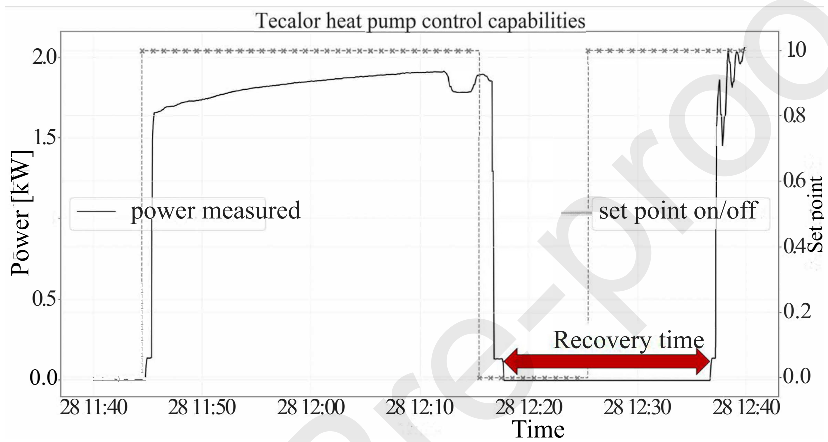

Figure 8 – Heat pump control capabilities analysis

Another test was performed to assess a stepwise activation. For certain flexibility services, a heat pump may have to deliver a linear increasing or decreasing power curve (e.g. track the TSO's aFRR signal). Since the modulation of the power output of the heat pumps was not possible, the test performed to deliver a linear ramp was based on stacking the deactivation of heat pumps. In this test, 1 minute between each heat pump switching on/off was set up, and a variation time of switching on between 5 to 30 minutes. During this test, 3 heat pumps were available at the case study pilot site. Temperature measurements of both the DHW and the floor heating system were available, allowing us to estimate the available flexibility in the system. The ranking of the heat pumps to switch them on and off was based on the measured temperature in the floor heating circuit, which turned out to be the limiting factor.

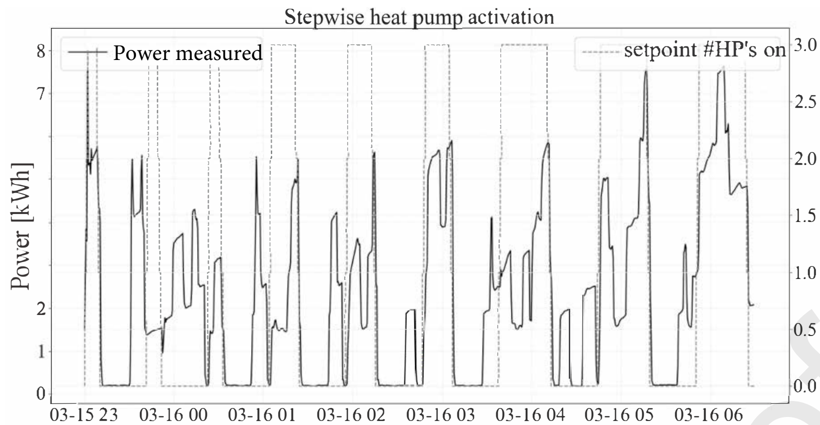

Figure 9 – Stepwise action of 3 heat pumps in the German pilot site

548 This test is shown in Figure 9. The results were not satisfactory to deliver a service such as aFRR standalone. This can be explained by the small pool (3 units) and the fact that the heat pumps were often unavailable for (de)activation due to comfort/safety constraints. Furthermore, since the heat pumps controls are driven by load curves that are dependent on the indoor and outdoor temperatures, and the latest was high for the testing period, the heat pump power demand was lower than initially expected. In Figure 10 a deeper zoom on the (un)availability causes of one of the heat pumps is shown. Number 1 indicates forced on the situation, which means unavailability of the heat pump. This is due to the DHW temperature dropping below a threshold, forcing the heat pump to switch on for comfort reasons. Number 2 indicates a forced off situation, which means the heat pump is unavailable because the floor heating temperature exceeds the threshold temperature, forcing the heat pump to switch off for comfort/safety reasons. After the temperature drops again below the low threshold, the heat pump can be activated again, as can be seen from the graph.

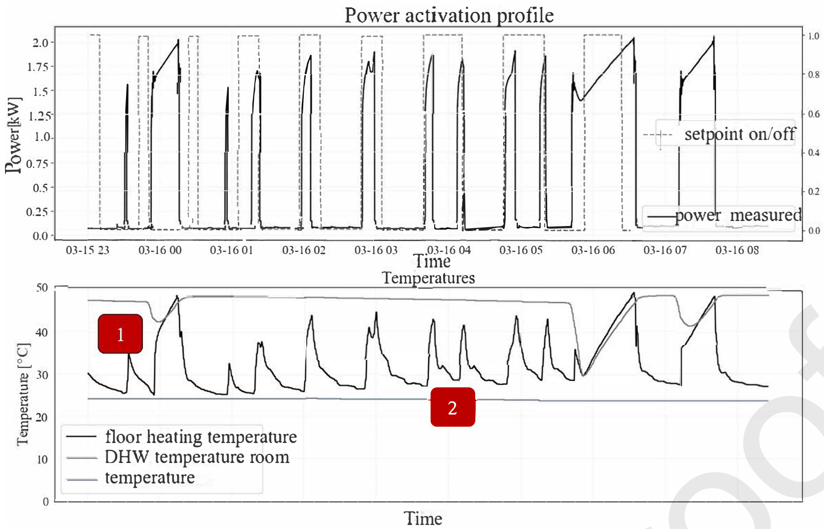

Figure 10 – Power and temperatures of the heat pump systems along the activation period

Looking at the overall results of the performed tests, it has been demonstrated that the flexible operation of heat pumps in the cases study is possible and can be leveraged for multiple flexibility services or energy markets. Nevertheless, important points of attention are: i) the latency to ramp up to full power to ramp down to switch it off, which is around 1 minute; ii) and the recovery time, which is around 20 minutes. Furthermore, the comfort set points and the available storage in hot water tanks or the inertia of the building clearly determine the duration for which the heat pump can be switched on or off.

4.2.1. Time series inputs for the flexibility model development

The operation of the case study in Wüstenrot, Germany, was a direct load control of four of the available heat pumps considering activation signals sent by a commercial aggregator. When activation was sent, the heat pumps had to operate for as long as possible during the whole activation period. In this case study, the control variable is the percentage of activation time (ON/OFF) of each building or heat pump (named 20, 22, 24 and 25). The energy flexibility is also analysed from this point of view. Figure 11 depicts the operation performance of the heat pumps from February 15th to March 31st. During those days, some activation signals were sent by the commercial aggregator. Therefore, as the actual heat pumps operation was affected by these signals, large differences between active power, P^e, and the forecasting of the baseline power in BaU scenario, P^b, can be appreciated for the activation period.

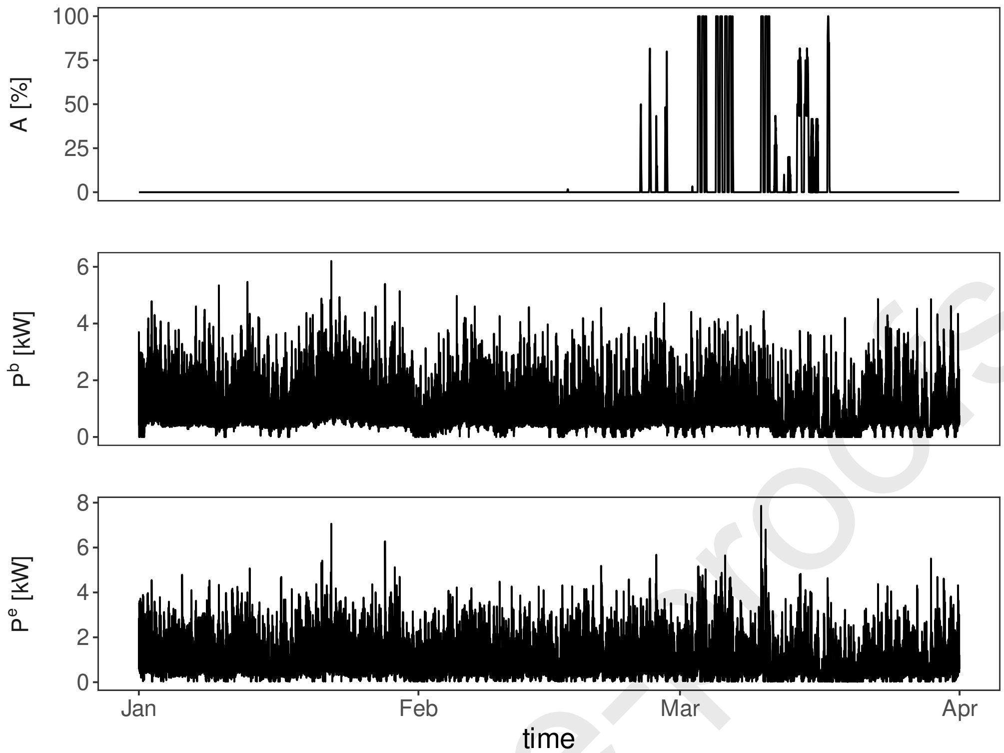

Figure 11 – Active heat pumps power (P^e), forecasting of baseline power in BaU scenario (P^b) and percentage of activation time in each hour (A) of four households in Wüstenrot pilot site
.

4.3. Operation of the Swiss case study

The use case in Naters, Switzerland, consists of a direct load control of five HPs that consider activation traces negotiated between the CM and the commercial aggregator. When an activation trace is accepted, the heat pumps should track the trace during the whole activation period.

Figure 12 represents the results of a day from a week-long test of direct load control services, detailed at the building level. The light grey vertical areas display the 15 minute negotiation periods between the aggregator and the CM. The light red vertical areas display the direct load control periods performed on-site as solutions of the tracking MPC optimization. It is not always easy to assess what a system would have done without direct load control, but coupling set points, temperature and power measurements can visually help. As a reminder, HP's local control works with hysteresis on the temperature of each storage. When the storage temperature drops too far below the setpoint value of the hysteresis, the compressor starts, and the HP runs until the upper value of the hysteresis is met. This is, of course the theory, but unforeseen events can sometimes change this behaviour.

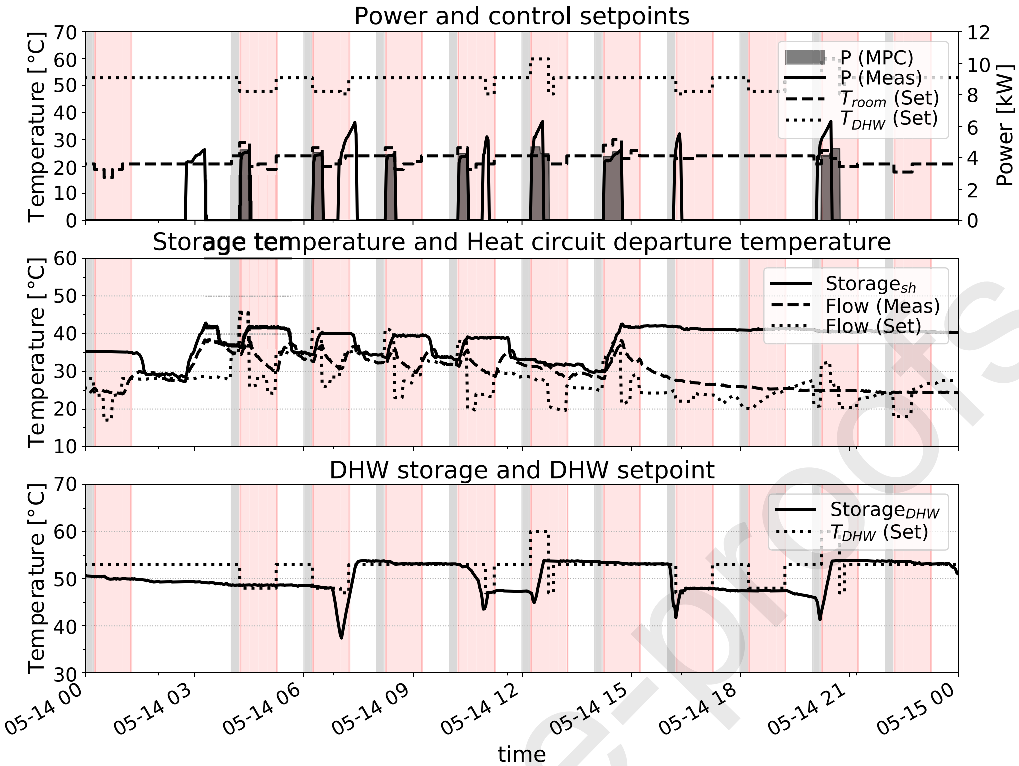

Figure 12 – Power and temperature variation resulting from direct load control for one building in the Swiss pilot site

The top panel of Figure 12 shows both the temperature setpoints used for controlling the HP and the power measurements. The dotted lines correspond to the setpoint values for SH and DHW, respectively. Outside the direct load control periods, the values of those set points are set back to their default values. The solid coloured line displays the measured power consumed by the compressor of the HP. The solid coloured bars are the power consumption given as the solution of the tracking MPC. The middle panel represents the effect of direct load control on SH. The dashed line corresponds to the measured departure temperature of the heating circuit after the 3-way valve. The dotted line represents the theoretical departure temperature of the circuit as given by the heat curve of the HP. It is modelled as a function of the SH setpoint displayed in the top panel and T_0 averaged over 3 hours. The bottom panel represents the effect of direct load control on DHW. In Figure 12, it can be seen that direct load control of SH perfectly matches the results of the tracking MPC. Instead, for the DHW load, it appears to be more difficult. Having only one sensor to assess the energy state inside the DHW storage tank makes it difficult to predict when a new cycle will occur. For comfort reasons, DHW is always prioritized and setpoints are only reduced to a minimum of 47 °C. Therefore, delaying a DHW cycle for more than 30 minutes is not always possible, as demonstrated for the DR call at 06:00. In the bottom panel, we can see that the storage temperature at the start of the period is low. This is because the setpoints are set to the lowest possible value. At 06:40, a DHW consumption brought the storage temperature below the lower bound of the hysteresis, which starts a new DHW cycle. The DR called at 10:00 is a good example of the usefulness of MPC when dealing with direct load control. When the power traces are generated, the storage tank temperature is maximal. There is only a small chance that a DHW cycle will happen in the next hour. However, within the third 15 minutes interval, a sudden high DHW consumption puts the storage temperature below the lower bound of the hysteresis, and the heat pump starts a new DHW cycle. At 11:00, to avoid deviating further from the trace, the DHW setpoint is reduced, which directly stops the heat pump.

4.3.1. Iterative tracking performance

Figure 13 presents the results of a day from a week-long test of direct load control services over all the HPs. The light grey vertical areas display the 15 minute negotiation periods between the aggregator and the CM. The light red vertical areas display the direct load control periods performed on-site as solutions of the tracking MPC optimization.

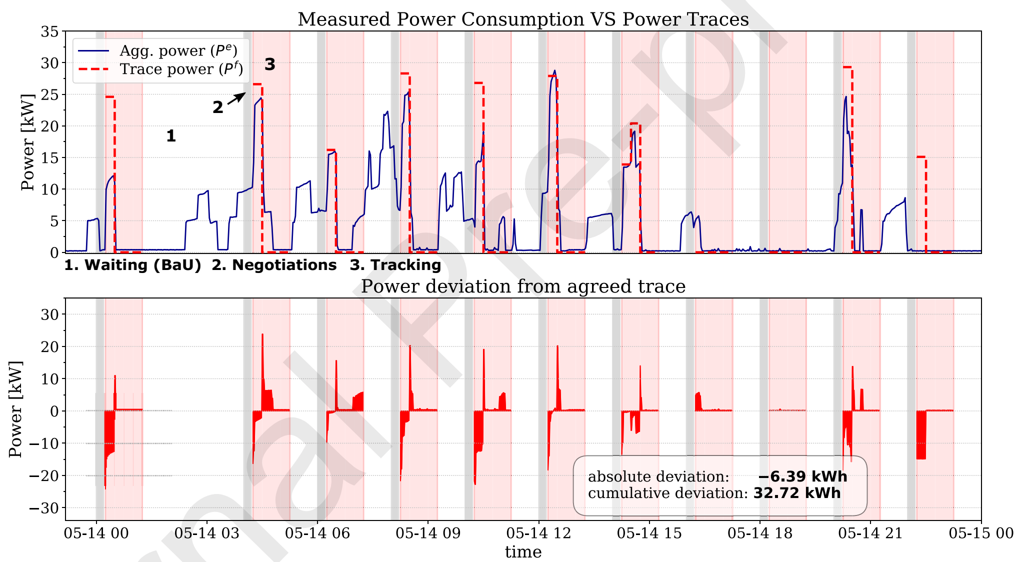

Figure 13 – Power deviation compared to the agreed-upon traces resulting from the DR calls over a day for a weekly test in the Swiss pilot site

.

The top panel of Figure 13 displays the aggregated power (blue) of five participating HPs on May 14^{th} 2020. The daily average outside temperature is 18 °C with temperatures above 20 °C from 12:00 to 20:00. Therefore, most HP consumption occurs during the early hours of the day when the outside temperature is still cold. The dashed red lines are the power loads P^f agreed upon by the aggregator and the CM. The selected traces are assumed to be constant over the sampling period of 15 minutes. Each one corresponds to a power trace resulting from a 6-hour forecast scheduling optimization problem proposed by the CM and selected by the aggregator. The bottom panel of Figure 13, represents the power deviation ($P^f - P^e$). When the values are negative, it means that the on-site power was lower than the expected trace, and when they are positive, it means that the power was higher. The relative deviation over the day is -6.4 kWh and the cumulative deviation, computed as the sum of all the absolute deviations, is equal to 32.7 kWh. When high power change occurs as a result of direct load control, high deviation spikes can be observed. The negative spikes correspond to an activation delay of the HPs: Even when conditions for the local controller are met, HP compressors are only started after a 2-minute delay by the local controller. To compensate, the tracking MPCs are launched two minutes before the new actuation periods. As soon as an optimal solution is found, the new setpoints are sent. Setpoints to switch off HPs are sent at the actuation time. HP compressors directly stop when conditions are met, except when an explicit minimum running time is implemented by the local controller. The positive spikes observed can be the result of the monitoring sampling rate of 2 minutes and of the way power is measured: The power consumption of four out of five HPs is not directly measured but reconstructed from operating temperature time series and manufacturer datasheets. The interpolation and the model formulation can sometimes create mismatches.

4.3.2. Time series inputs for the flexibility model development

In this use case, the objective of the flexibility function is to characterize how flexible the HP consumption was due to the activation trace accepted by both entities in terms of amount and shift in time. In this case study, the control variables are the DHW and SH setpoint temperature of five multi-household buildings. The entity that controls these variables is the CM, which proposes feasible traces that can be fulfilled. Figure 14 depicts the performance of the HPs from April 3rd to May 15th. The granularity of the monitored data is two minutes, and the power is aggregated over the individual readings of the five available buildings. For this field operation period, multiple activation traces were tested in several operation tests. They are represented separated by gaps in Figure 14. In the top panel, the difference between the power trace to be tracked and the baseline forecasting is represented. As expected, significant differences between these two time series are clearly appreciated. The middle panel shows the differences between the active power, P^e, and forecasting of the baseline power,P^b. As in the other graph, the differences show that the heat pumps are following the trace up to a certain level and that these traces have very different patterns than the BaU scenario.

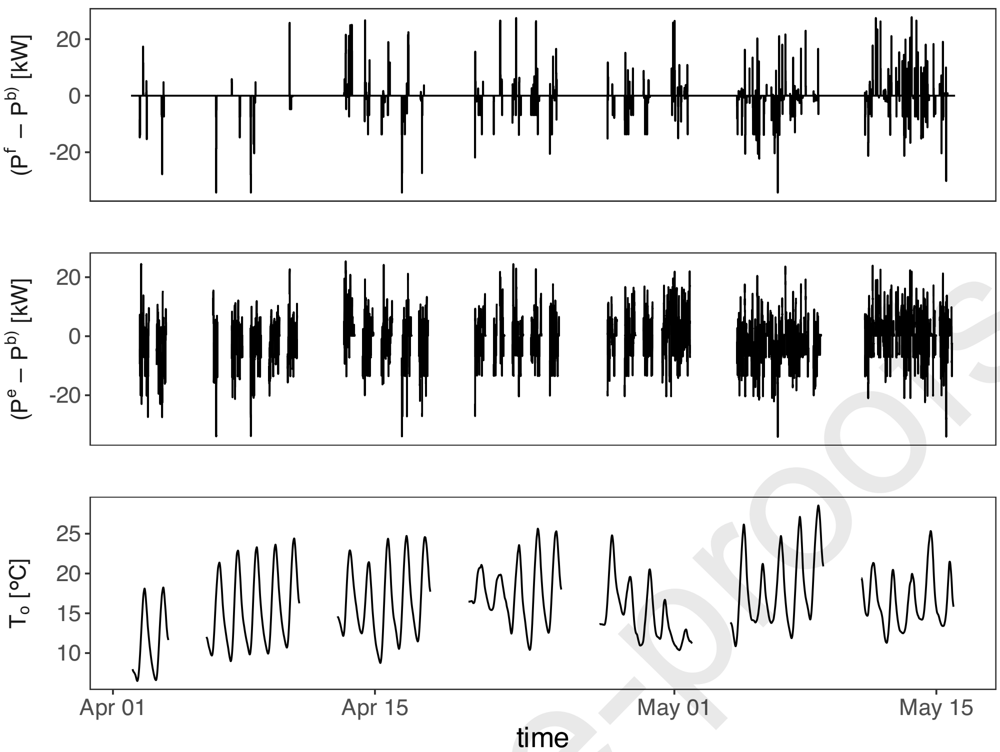

Figure 14 – Difference between the trace to be tracked, P^f, and the prediction of the baseline, P^b, versus the difference between the active power P^e and the baseline prediction of the baseline, P^b, and the 4-hour moving-averaged outdoor temperature in the Swiss pilot site. The tests in May were week-long tests
.

4.4. Energy flexibility evaluation and quantification

4.4.1. Training and validation of the flexibility models

For the case study where the activation variable is the Spanish day-ahead electricity price, a training and validation activation period was set up from March 29th to April 12th 2020. The flexibility model of this case study is defined in Equation 1. The training of the model to identify the regression parameters was carried out using 90 % of the data. The remaining 10 % of data was used to validate the model with new data and then avoid model overfitting. The Flexibility Function (FF) is finally inferred from this model. The top plot of Figure 15 depicts the training and validation periods with white and grey backgrounds, respectively. In this plot, the active power, P^e, is represented by a black coloured line. The forecasting based on the flexibility model is represented by a red coloured line. It can be seen that no significant differences in residuals between the two periods are appreciated; therefore, it is confirmed that overfitting issues were avoided. Additionally, from the two bottom plots, the Auto Correlation Function, ACF, and the Partial Autocorrelation Function, PACF, of the residuals of the training period, do not indicate autocorrelation in residuals. Therefore, they can be considered i.i.d, and the white noise condition is fulfilled. This is the requirement for a model to be considered valid.

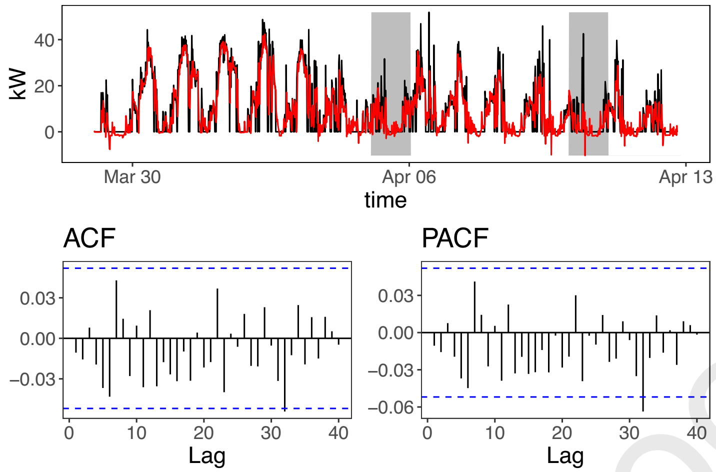

Figure 15 – Flexibility model for the Spanish pilot site: the upper graph is a comparison of the active power (black line) and the predicted one (red line); the lower graphs show the autocorrelation functions of the training period residuals

For the case study where the activation variable is the percentage of activation time, in the German pilot case, a training and validation activation period was set up from February 15th to March 31st 2020. The flexibility model of this case study is defined in Equation 2. The training of the model was carried out using 90 % of the data. The remaining 10 % of the data was used to validate the model. In Figure 16, the upper graph depicts the training and validation periods with white and grey backgrounds, respectively. In this graph, the active power, P^e, is represented by a black coloured line. The forecasting based on the flexibility model is represented by a red coloured line. It can be seen that no significant differences in residuals between the two periods are appreciated. Although there are two significant spikes in time lags 3 and 12 in the bottom plots of the ACF and PACF, there is no clear indication of autocorrelation in residuals of the training period. Therefore, they can be considered as i.i.d. and then, the white noise condition is fulfilled for this flexibility model.

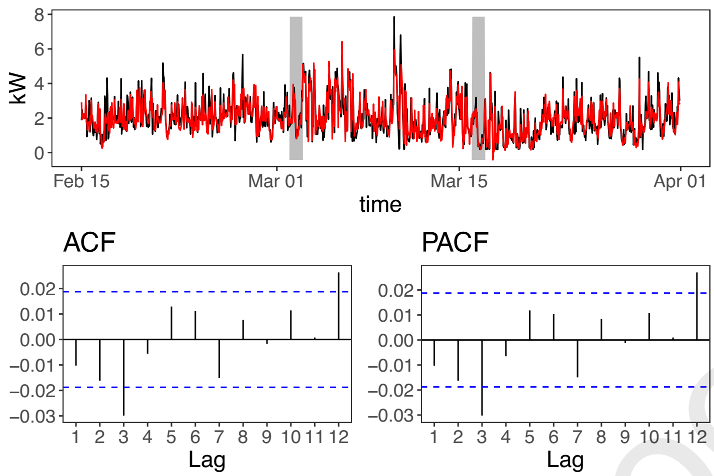

Figure 16 – Flexibility model for the German pilot site; the upper graph shows a comparison of the active power (black line) and the predicted one (red line); the lower graphs show the autocorrelation functions of the training period residuals

.

For the case study where the activation variable is the trace to be tracked, the Swiss pilot case, a training and validation activation period was set up from April 3rd to May 15th in the Swiss pilot site case study. The flexibility model of this case study is defined in Equation 3. The training of the model was carried out using 90 % of the data. The remaining 10 % of data was used to validate that the model. In Figure 17, the upper graph depicts the training and validation periods with white and grey backgrounds, respectively. In this graph, the difference between the active power and the prediction of the baseline power in BaU, $(P^e - P^b)$, is represented by a black coloured line. The forecasting based on the flexibility model is represented by a red coloured line. It can be seen that no significant differences in residuals are appreciated. Although there is one significant spike in time lag 15, in the bottom plots of the ACF and PACF, there is no clear indication of autocorrelation in residuals of the training period. Therefore, they can be considered i.i.d. The white noise condition is fulfilled for this flexibility model.

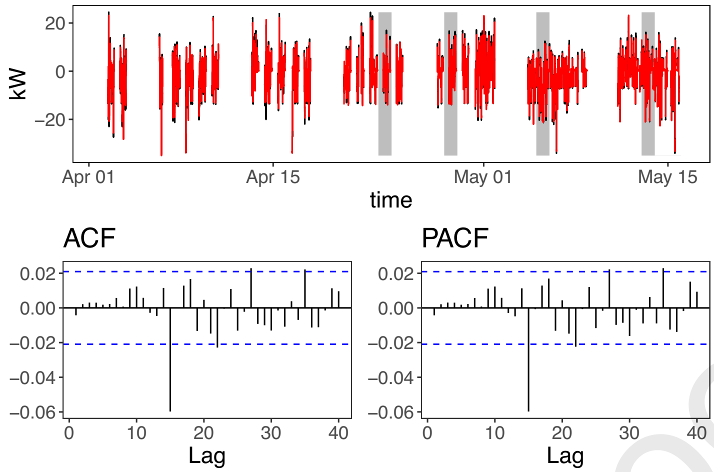

Figure 17 – Flexibility model for the Swiss pilot site; the upper graph shows a comparison of $(P^e - P^b)$ (black line) and the predicted one performed with the flexibility model (red line); the lower graphs show the autocorrelation functions of the training period residuals

.

4.4.2. *Flexibility functions*

Figure 18 and Figure 19 show the obtained flexibility functions, FFs, for the Spanish case study, where the activation variable is the electricity day-ahead Spanish spot market. The activation variable, the day-ahead electricity price, is normalized to activation and deactivation signals of 10 cents. Figure 18 shows the obtained FFs due to positive signals of different lengths and two different outdoor temperature levels. The left column shows the FFs for outdoor temperature ranges between 6.67 ºC and 12.3 ºC. The right column shows the FFs for outdoor temperature ranges between 12.3 ºC and 21.5 ºC. It can be seen that the flexibility decreases for low outdoor temperature ranges. When outdoor temperatures are between 6.67 ºC and 12.3 ºC, the average maximum deactivated power reaches -7 kW, and it remains for the first 30 minutes. Then, it increases to -3.5 kW from 30 to 45 minutes, and finally, it linearly increases to -1 kW after 100 minutes of the initial price change. Whereas, when outdoor temperatures are between 12.3 ºC and 21.5 ºC, the maximum deactivated power reaches -11 kW for the first 15 minutes; it decreases to -14 kW after 30 minutes, and finally, it increases up to -1 kW after 100 minutes of the price change. The rebound effect achieves the same maximum power levels for both temperature ranges but in positive. They start just when the activation signal finishes and reach the maximum level within the first 30 minutes after the activation signal ends. Considering the maximum available power of the two heat pumps of 60 kW, this represents maximum flexibility between 11 % and 23 %, with a rebound of the same level, for low and high outdoor temperature ranges, respectively. It can also be concluded that the estimated period where major energy shifts could be done is the starting 30 minutes after the price signal is triggered, in both outdoor temperature ranges. This conclusion is closely related to the thermal capacity of the water storage tank, which is 3,500 litres, and the permitted water tank temperature variation, which is constrained by the indoor comfort conditions in the offices, shops and the local food market.

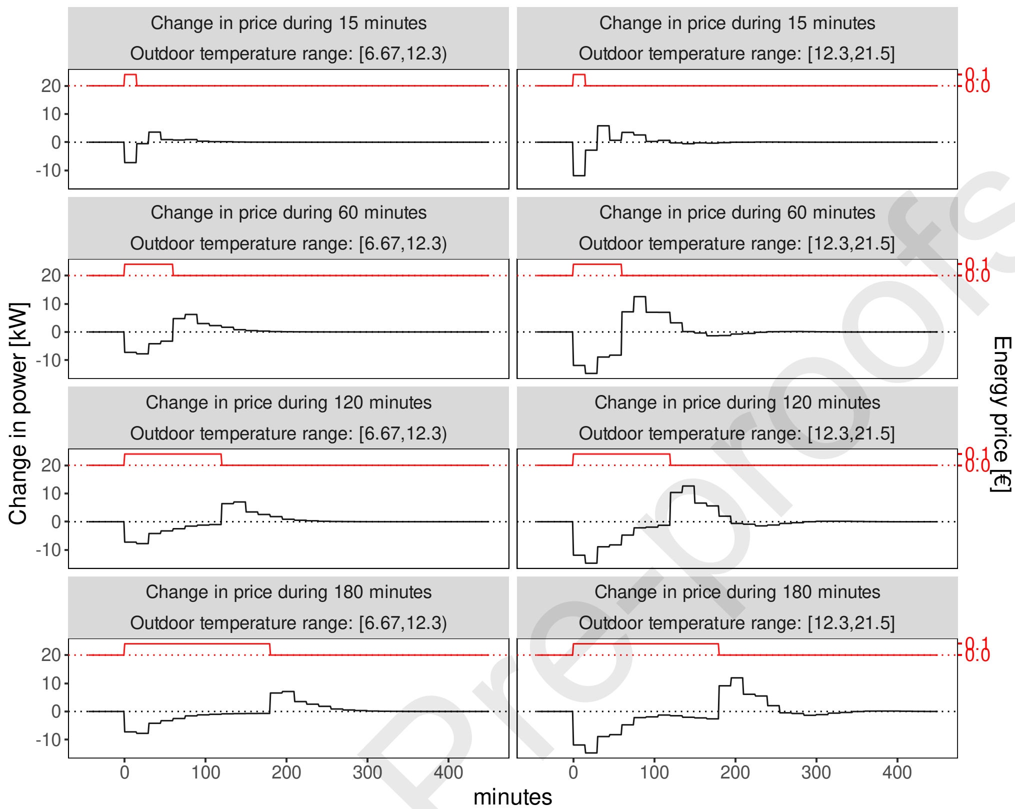

Figure 18 – *FFs* of the Spanish case study for positive changes of the spot market price

Figure 19 depicts the obtained *FFs* due to negative signals of different lengths and the same outdoor temperature levels. The flexibility performance is identical to the case of positive activation but another way around. The rebound effect achieves the same maximum power levels for both temperature ranges but in negative. The same conclusions as in the case of positive signals can be deducted.

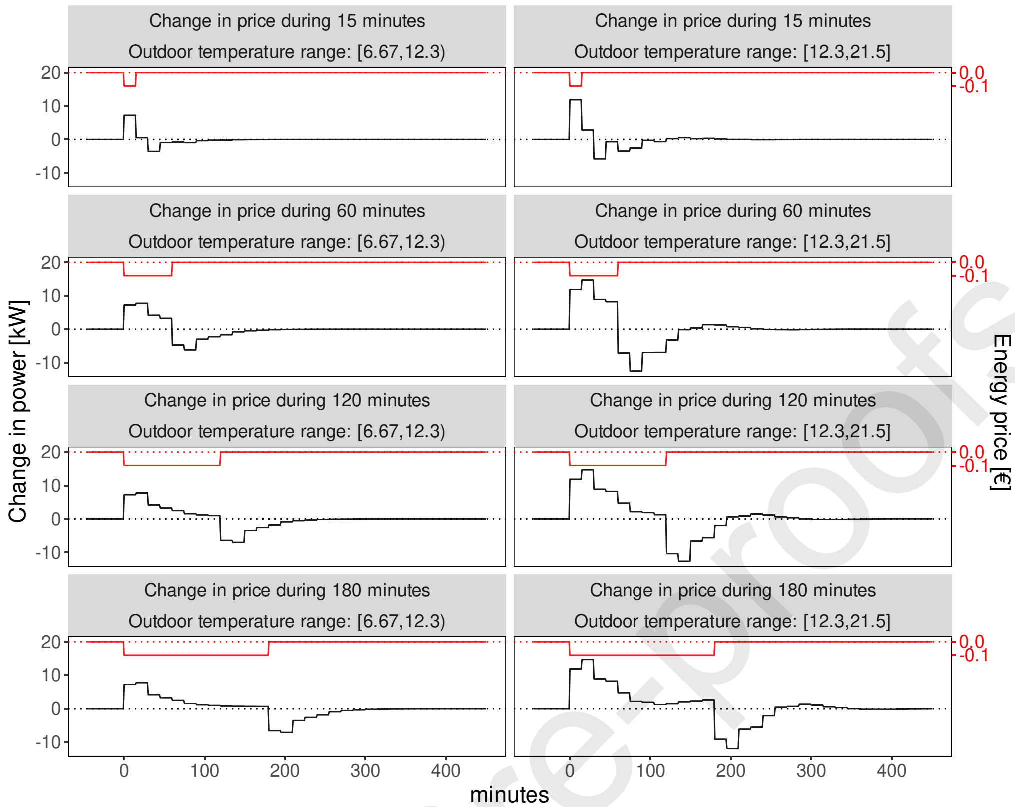

Figure 19 – FFs of the Spanish case study for negative changes of the spot market price

Figure 20 shows the Flexibility Functions, FFs of four heat pumps and their aggregated power, of the case study where the activation signal is the percentage of activation within an activation period. The activation variable has been normalized to 100 % activation time. The Figure 20 represents the FFs of each heat pump/building, named as 20, 22, 24 and 25 in the legend, and the aggregated flexibility of all of them, named as ”all” in the legend. Every plot shows a FF for several activation periods ranging from 1 h to 4 h. From this Figure, multiple insights in relation to the achieved flexibility of a cluster of heat pumps can be extracted. The total amount of power flexibility for the cluster of 4 buildings reaches 2.8 kW -on average- for the first hour of activation. And from there, it decreases to 2.3 kW for the second and the third hours of activation. If the activation period is extended to four hours, maximum flexibility decreases to 2 kW. Considering a maximum available power of the four heat pumps of 10.9 kW, this represents maximum flexibility of 25 % for the first hour, 20 % for three hours and 18 % for four hours. After the activation periods, Figure 20 depicts a long wave rebound effect of about 20 % of the total active power. Nonetheless, around 70 % of this rebound takes place within the first 3 h after the activation period ends.

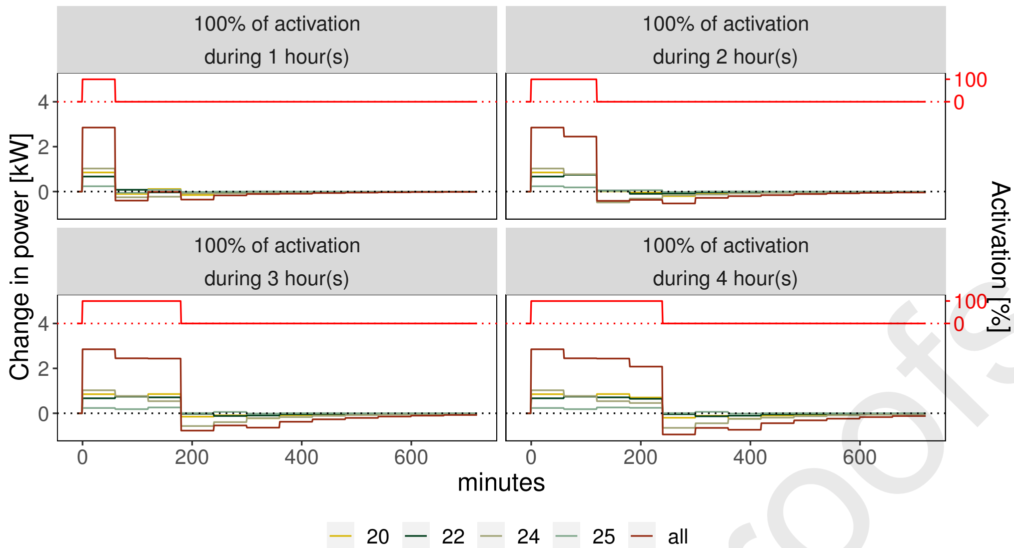

Figure 20 – *FFs* of 4 heat pumps of the German case study

In Figure 20, it can also be seen that the reactions of buildings 20, 22 and 24 are quite similar and also very similar to the aggregated *FFs*. However, a very different behaviour happens in building 25 since it seems this heat pump is not activated. This may be due to less flexible indoor comfort conditions.

Figure 21 shows the *FFs* for the swiss case study. In this case, the activation variable is a power trace that should be tracked, and the flexibility is assessed as the deviation towards the traces and towards de predicted baseline in the BaU scenario. In Figure 21, the left Y-axis describes the change in power $(P^e - P^b)$ and the right Y-axis describes the change in power due to the trace negotiated with the commercial aggregator $(P^f - P^b)$. The flexibility is analysed for two different outdoor temperature levels; low-to-mid range [6.5 ºC, 15.7 ºC] in yellow and mid-to-high [15.7 ºC, 28.5 ºC] in black. Two types of normalized activation traces of 1 kW (e.g. red signal [-1, 0, 1]) are tested: (1) *Negative*, when the consumption is lower than the baseline, and (2) *Positive*, when the consumption is higher than the baseline. The terms *Negative* and *Positive* used here have to be differentiated from the existing positive (Upward) and negative (Downward) reserve services defined in the market regulation and provided by conventional generators. In this methodology, the term *Positive* refers to an increase in power consumption compared to the baseline, which, from a market perspective, is equivalent to a decrease in power production (negative reserve).

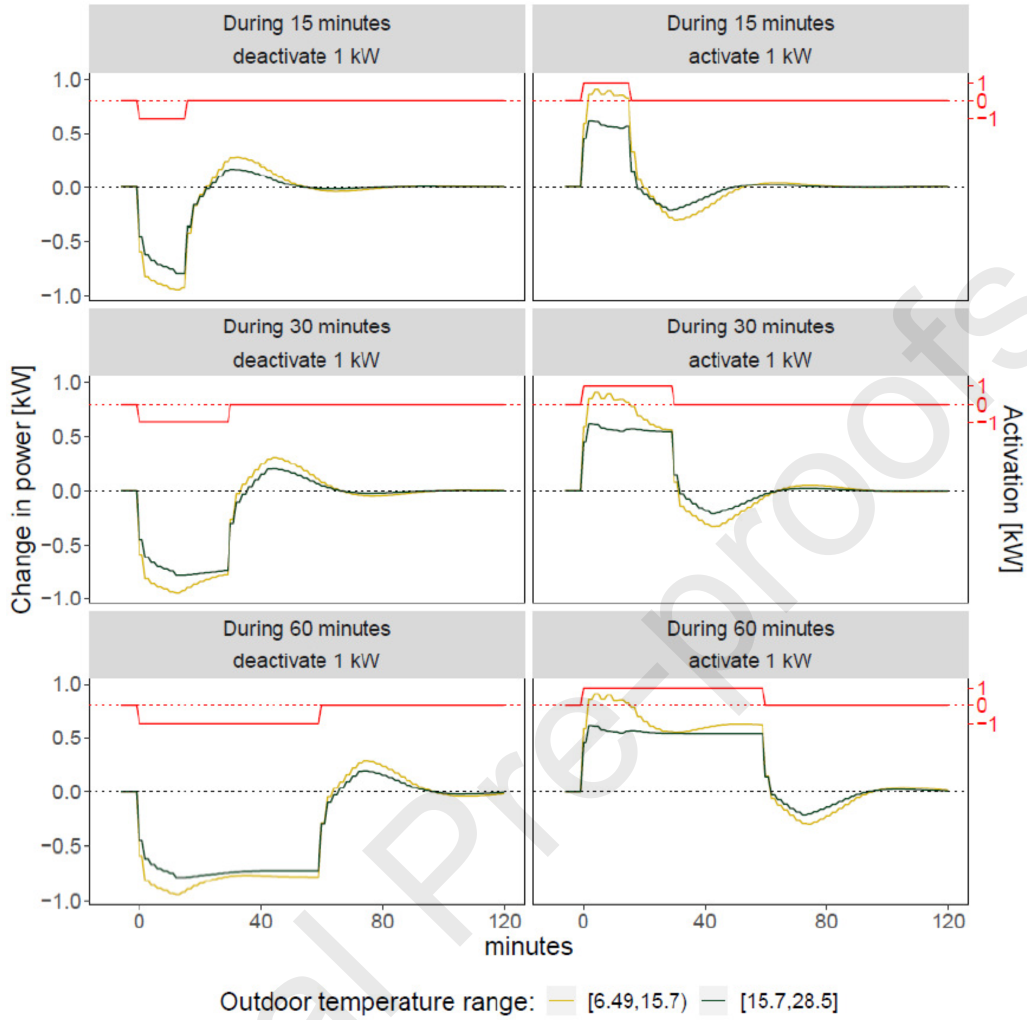

Figure 21 – Flexibility Function (FF) of a 5-buildings cluster in Naters

In the case of tracking *negative* activation traces (left panels) in low-to-mid outdoor temperature levels (yellow lines), the active power follows 80 to 90 % of the power trace to be tracked for the first 15 minutes, reaching the maximum deactivation peak (98 %) after 13 minutes. Then, the deactivation decreases to 75 % after 30 minutes, maintaining this percentage for 30 minutes more. When tracking a *positive* activation trace, the actual power follows 80-90% of the theoretical activation for the first 15 minutes, then, it linearly decreases to 50 % after 30 minutes and maintains this percentage, with a small rebound (+10 %), up to the 60 minutes. This means that heat pumps involved in this case study, when the outdoor temperature is in the low-to-mid range, can provide the amount of flexibility required by the commercial aggregator for the first 15 minutes. Still, then, the limited availability of thermal energy storage in the building (either for SH or DHW) does not allow for full activation compliance. In both outdoor temperature levels, the rebound effect reaches up to 30 % change in power. It starts just after the activation/deactivation of the trace, and its peak is after approximately 13 minutes. In the case of mid-to-high outdoor temperatures levels, the flexibility peak of the first 15 minutes no longer exists in both *negative* and *positive* traces to be tracked. This can be explained mainly because at these temperature levels; the buildings have less thermal storage capacity and hence less energy flexibility to keep the indoor comfort within the user-defined comfort boundaries. In this case, the system which can still provide a certain level of flexibility is the DHW system, which is thermostatically controlled by the water tank temperature set points. The average compliance of tracking the trace is 60 % along the 60 minutes of activation in the case of positive and 75 % in the case of negative traces. The rebound effects follow the same path as in the lower temperatures case but with smaller peaks of around 25 % of the change in power.

5. Discussion

Some specific conclusions can be drawn from the operation of the DR services in each of the three pilot sites:

- The direct load control of the heat pumps of the Spanish pilot site achieved 18 % of accumulated cost savings at the end of the testing period (2 weeks). This is a promising result to demonstrate the benefits of optimising the operational costs of heat pumps through augmented performance with price information from the wholesale market forecast data.
- In the German pilot site, it was demonstrated that using the flexibility of the heat pumps allowed to optimize the heating energy cost on the day-ahead energy market. This flexibility also enabled balancing a BRP's portfolio and optimization on the balancing market. With a limited number of heat pump assets and only ON/OFF control, it was impossible to deliver linear power ramps based on the stacking of heat pumps.
- In the Swiss pilot site, a success of 91 % heat pump activation for the transactive DR approach and 50-95 % fulfilment of the activation traces was achieved for the testing period. The results are strongly correlated with the external temperature. Mid-range outdoor temperature conditions offered more flexibility, as highlighted by the higher activation success and the *FF* closer to 100 % of the theoretical activation.

The developed standard methodology for assessing the flexibility allowed to compare results from the different DR use cases and gave the necessary support for cross-comparison of the most significant energy flexibility indicators. Some specific conclusions can be deducted for the achieved flexibility in each pilot site:

5.1. Spanish case study

Considering the peak power of the heat pump system, the maximum flexibility achieved was between 11 % and 23 %, depending on low or high outdoor temperature ranges, respectively. A contrary rebound effect at the same level was achieved in both cases. Table 1 summarizes the achieved active flexibility for this pilot site:

Table 1 – Achieved active power and rebound effect defined by the *FF* in the Spanish use case

Activation time [min]	Maximum change in power [kW]	Maximum power rebound [kW]
Flexibility with low outdoor temperature [6.6 °C ≤ T ≤ 12.3 °C]		
positive/negative change of price		
t ≤ 30	-7/7	6/-6
30≤ t ≤ 45	-3.5/3.5	3/-3
45≤ t ≤ 100	linear increase	linear decay
t > 100	-1/1	0.8/-0.8
Flexibility with high outdoor temperature [12.3 °C ≤ T ≤ 21.5 °C]		
Positive/negative change of price		
t ≤ 15	-11/11	8/-8
t ≤ 30	-14/14	12/-12
30≤ t ≤ 45	-8/8	6/-6
45≤ t ≤ 100	linear increase	linear decay
t > 100	-1/1	0.8/-0.8

5.2. *German case study*

In the German pilot site, considering a maximum aggregated power of 10.9 kW, 25 % of flexibility was achieved for the first hour. For activation of three hours, it was reduced to 20 %, and it finally decreased to 18 % for activation of four hours. A long wave rebound effect of about 20 % of the total activated power appears in all cases. However, around 70 % of the total rebound effect occurs within the first 3 h after the activation period ends. Table 2 summarizes achieved active flexibility for this pilot site:

Table 2 – Achieved active power and rebound effect defined by the *FF* in the German use case

Activation time [min]	Maximum change in power [kW]	Maximum power rebound [kW]
Flexibility under a 100 % positive activation signal		
t ≤ 60	2.8	-0.8
60≤ t ≤ 180	2.3	-0.5
180≤ t ≤ 240	2	exponential increase
t > 240	—-	0.0

5.3. *Swiss case study*

The heat pumps involved in the Swiss case study can provide the amount of flexibility required by the commercial aggregator for the first 15 minutes. Still, then, the limited availability of thermal energy storage in the buildings does not allow for full activation compliance. In both outdoor temperature levels, the rebound effect reaches up to 30 % change in power. The average compliance of tracking the trace is 60 % along the 60 minutes of activation in the case of positive activation traces and 75 % in the case of negative ones. Table 3 summarises the achieved active flexibility for this pilot site:

Table 3 – Achieved active power and rebound effect defined by the *FF* in the Swiss use case

Activation time [min]	Maximum change in power [%]	Maximum power rebound [%]
Flexibility with low outdoor temperature [6.49 °C ≤ T ≤ 15.7 °C]		
positive/negative trace to be followed		
t ≤ 15	85/-98	-40/40
15≤ t ≤ 30	linear decrease/-75	linear increase / linear decay
30≤ t ≤ 60	60/-75	0/0
Flexibility with high outdoor temperature [15.7 °C ≤ T ≤ 28.5 °C]		
Positive/negative change of price		
t ≤ 15	60/-75	-25/25
15≤ t ≤ 30	60/-75	linear increase / linear decay
30≤ t ≤ 60	60/-75	0/0

6. Conclusions

This study confirms that thermostatically controlled heat pumps represent a huge potential for DR flexibility. Furthermore, it is possible to manage clusters of heat pumps to respond to requests for DR flexibility. In addition, it has been proven that forecasting and optimization algorithms can be tailored to the particularities of each system configuration (e.g. HP interface, HP installation, and temperature sensors).

The operation tests performed in three European pilot sites demonstrated that the flexible operation of heat pumps in the field is possible and can be leveraged for multiple flexibility services or energy markets. However, several problems need to be addressed with most legacy systems. In general, those systems do not provide fully interoperable connectivity with the heat pump, resulting in constraints to the control and less flexible systems. Additionally, it has been confirmed that outdoor conditions, configured set points and the available thermal storage, both in hot water tanks or inertia in the building, determine the duration for which the heat pump can be switched on or off. Another important conclusion from this research is that a new player, called the Cluster Manager (CM), is essential to assure a successful operation of the DR services in real market scenarios.

7. Future work

Although the developed methodology to assess the flexibility in the different pilot sites shows promising outcomes to demonstrate its scalability and wider application, some procedures' limitations to determine the *FF* need further research. These limitations are mainly related to the non-accurate incorporation of the dynamic variability of the flexibility and the dependencies between the active energy and the activation variable. Both have been addressed in this research by including the autoregressive terms in the model. However, this procedure is not accurate enough and can miss some of the nonlinearities. Therefore, some improvements should be addressed. As an example, recent papers [21] opened alternative methodologies to address these non-linearities in price-based DR schemes. These complementary approaches should be investigated in real practice experiences. Finally, simpler and more cost-efficient computational methods to evaluate the flexibility potential of large amounts of buildings and HVAC systems need to be further developed to assure a seamless connection with commercial practices of aggregators and cluster managers in already existing European energy flexible markets.

8. Acknowledgements

This work emanated from research conducted with the financial support of the European Commission through the H2020 project Sim4Blocks, grant agreement 695965. Dr. J. Cipriano thanks the Ministerio de Ciencia e Innovación for the Juan de la Cierva Incorporación grant.

References

[1] C. Lo and N. Ansari, "Decentralized Controls and Communications for Autonomous Distribution Networks in Smart Grid," IEEE Transactions on Smart Grid, vol. 4, pp. 66–77, Mar. 2013. Conference Name: IEEE Transactions on Smart Grid.

[2] P. D. Lund, J. Lindgren, J. Mikkola, and J. Salpakari, "Review of energy system flexibility measures to enable high levels of variable renewable electricity," Renewable and Sustainable Energy Reviews, vol. 45, pp. 785–807, May 2015.

[3] D. S. Kirschen, A. Rosso, J. Ma, and L. F. Ochoa, "Flexibility from the demand side," in 2012 IEEE Power and Energy Society General Meeting, pp. 1–6, July 2012. ISSN: 1944-9925.

[4] S. Weitemeyer, D. Kleinhans, T. Vogt, and C. Agert, "Integration of Renewable Energy Sources in future power systems: The role of storage," Renewable Energy, vol. 75, pp. 14–20, Mar. 2015.

[5] P. Denholm, E. Ela, B. Kirby, and M. Milligan, "Role of Energy Storage with Renewable Electricity Generation," Tech. Rep. NREL/TP-6A2-47187, National Renewable Energy Lab. (NREL), Golden, CO (United States), Jan. 2010.

[6] P. Siano, "Demand response and smart grids—A survey," Renewable and Sustainable Energy Reviews, vol. 30, pp. 461–478, Feb. 2014.

[7] V. Giordano, A. Meletiou, C. Felix, A. Mengolini, M. Ardelean, G. Fulli, M. Sánchez, and C. Filiou, "Smart grid projects in Europe: lessons learned and current developments 2012 update. .," 2013.

[8] Z. Ma, J. D. Billanes, and B. N. Jørgensen, "Aggregation Potentials for Buildings—Business Models of Demand Response and Virtual Power Plants," Energies, vol. 10, p. 1646, Oct. 2017. Number: 10 Publisher: Multidisciplinary Digital Publishing Institute.

[9] X. Cao, X. Dai, and J. Liu, "Building energy-consumption status worldwide and the state-of-the-art technologies for zero-energy buildings during the past decade," Energy and Buildings, vol. 128, pp. 198–213, Sept. 2016.

[10] T. M. Lawrence, M.-C. Boudreau, L. Helsen, G. Henze, J. Mohammadpour, D. Noonan, D. Patteeuw, S. Pless, and R. T. Watson, "Ten questions concerning integrating smart buildings into the smart grid," Building and Environment, vol. 108, pp. 273–283, Nov. 2016.

[11] G. Serale, M. Fiorentini, A. Capozzoli, D. Bernardini, and A. Bemporad, "Model Predictive Control (MPC) for Enhancing Building and HVAC System Energy Efficiency: Problem Formulation, Applications and Opportunities," Energies, vol. 11, p. 631, Mar. 2018. Number: 3 Publisher: Multidisciplinary Digital Publishing Institute.

[12] P. Kohlhepp, H. Harb, H. Wolisz, S. Waczowicz, D. Müller, and V. Hagenmeyer, "Large-scale grid integration of residential thermal energy storages as demand-side flexibility resource: A review of international field studies," Renewable and Sustainable Energy Reviews, vol. 101, pp. 527–547, Mar. 2019.

[13] J. L. Boudec and D. Tomozei, "Demand response using service curves," in 2011 2nd IEEE PES International Conference and Exhibition on Innovative Smart Grid Technologies, pp. 1–8, Dec. 2011. ISSN: 2165-4824.

[14] C. Eid, P. Codani, Y. Perez, J. Reneses, and R. Hakvoort, "Managing electric flexibility from Distributed Energy Resources: A review of incentives for market design," Renewable and Sustainable Energy Reviews, vol. 64, pp. 237–247, Oct. 2016.

[15] A. Arteconi, A. Mugnini, and F. Polonara, "Energy flexible buildings: A methodology for rating the flexibility performance of buildings with electric heating and cooling systems," Applied Energy, vol. 251, p. 113387, Oct. 2019.

[16] C. Finck, R. Li, R. Kramer, and W. Zeiler, "Quantifying demand flexibility of power-to-heat and thermal energy storage in the control of building heating systems," Applied Energy, vol. 209, pp. 409–425, Jan. 2018.

[17] G. Reynders, R. Amaral Lopes, A. Marszal-Pomianowska, D. Aelenei, J. Martins, and D. Saelens, "Energy flexible buildings: An evaluation

of definitions and quantification methodologies applied to thermal storage," Energy and Buildings, vol. 166, pp. 372–390, May 2018.

[18] R. El Geneidy and B. Howard, "Contracted energy flexibility characteristics of communities: Analysis of a control strategy for demand response," Applied Energy, vol. 263, p. 114600, Apr. 2020.

[19] A. Bampoulas, M. Saffari, F. Pallonetto, E. Mangina, and D. P. Finn, "A fundamental unified framework to quantify and characterise energy flexibility of residential buildings with multiple electrical and thermal energy systems," Applied Energy, vol. 282, p. 116096, Jan. 2021.

[20] R. G. Junker, A. G. Azar, R. A. Lopes, K. B. Lindberg, G. Reynders, R. Relan, and H. Madsen, "Characterizing the energy flexibility of buildings and districts," Applied Energy, vol. 225, pp. 175–182, Sept. 2018.

[21] R. G. Junker, C. S. Kallesøe, J. P. Real, B. Howard, R. A. Lopes, and H. Madsen, "Stochastic nonlinear modelling and application of price-based energy flexibility," Applied Energy, vol. 275, p. 115096, Oct. 2020.

[22] "Was ist der Intraday-Handel von Strom?. https://www.next-kraftwerke.de/wissen/intraday-handel," May 2014.

[23] "Regelenergie & Regelleistung - was ist das?. https://www.next-kraftwerke.de/wissen/regelenergie," Nov. 2010.

[24] "Regelenergiemarkt im Umbruch II – von Preisspitzen zum Mischpreisverfahren. https://blog.energybrainpool.com/regelenergiemarkt-im-umbruch-ii-von-preisspitzen-zum-mischpreisverfahren/," Feb. 2020.

[25] "Day-Ahead-Handel - was ist das?. https://www.next-kraftwerke.de/wissen/day-ahead-handel," 2014.

[26] "What is Intraday Trading?. https://www.next-kraftwerke.be/en/knowledge-hub/intraday-trading/."

[27] F. Ocker, S. Braun, and C. Will, "Design of European balancing power markets," in 2016 13th International Conference on the European Energy Market (EEM), pp. 1–6, June 2016. ISSN: 2165-4093.

[28] M. D. Galus, "Smart grid roadmap and regulation approaches in Switzerland," CIRED - Open Access Proceedings Journal, vol. 2017, pp. 2906–2909, Oct. 2017. Publisher: IET Digital Library.

[29] J. Cipriano, G. Mor, D. Chemisana, D. Pérez, G. Gamboa, and X. Cipriano, "Evaluation of a multi-stage guided search approach for the calibration of building energy simulation models," Energy and Buildings. ENB-D-14-01064R1.

[30] P. Bacher and H. Madsen, "Identifying suitable models for the heat dynamics of buildings," Energy and Buildings, vol. 43, pp. 1511–1522, 2011.

[31] P. Bacher, H. Madsen, H. A. Nielsen, and B. Perers, "Short-term heat load forecasting for single family houses," Energy and Buildings, vol. 65, pp. 101–112, Oct. 2013. 00045.

[32] B. Grillone, S. Danov, A. Sumper, J. Cipriano, and G. Mor, "A review of deterministic and data-driven methods to quantify energy efficiency savings and to predict retrofitting scenarios in buildings," Renewable and Sustainable Energy Reviews, vol. 131, p. 110027, Oct. 2020.

[33] F. Amblard, J. Page, R. Parakkal Menon, M. Brennenstuhl, and J. Cipriano, "D.3.1-Optimization strategies for the use case scenarios. SIM4BLOCKS H2020 project. Grant agreement n° 695965.," Tech. Rep. Deliverable D.3.1., SIm4Blocks project, 2018.

[34] T. Hastie and R. Tibshirani, "Generalized additive models," p. 10, 1990.

[35] F. D'Ettorre, M. Brennenstuhl, A. Kathirgamanathan, M. D. Rosa, M. Yadack, U. Eicker, and D. P. Finn, "A set of comprehensive indicators to assess energy flexibility: a case study for residential buildings," E3S Web of Conferences, vol. 111, p. 04044, 2019. Publisher: EDP Sciences.

[36] L. Romero Rodríguez, M. Brennenstuhl, M. Yadack, P. Boch, and U. Eicker, "Heuristic optimization of clusters of heat pumps: A simulation and case study of residential frequency reserve," Applied Energy, vol. 233-234, pp. 943–958, Jan. 2019.

[37] T. Schütz, H. Harb, R. Streblow, and D. Müller, "Comparison of models for thermal energy storage units and heat pumps in mixed integer linear programming. ECOS 2015-28th International Conference on Efficiency, Cost, Optimization, Simulation and Environmental Impact of Energy Systems.," (Pau, France), July 2015.